Six5 results in down-regulation of myogenin, without altering MyoD and Pax7 expression, suggesting that overproduction of Six4 or Six5 negatively regulates the differentiation of satellite cells by repressing the expression of myogenin, while they do not affect the activation of these cells.

Six5 knockdown promotes proliferation of muscle satellite cells

We also examined the functions of *Six* genes using the Stealth small interfering RNA (siRNA)-mediated knockdown approach. The knockdown efficiency of each siRNA against individual *Six* genes, *Six1*, *Six4* and *Six5*, was validated in C2C12 cell line (Supplementary Fig. 2). In muscle satellite cells derived from the extensor digitorum longus (EDL) of 8- to 12-week-old wild-type mice, the endogenous level of Six proteins was not affected by the transfection of negative control siRNA (Fig. 6A, data not shown). The use of Six1 siRNA, Six4 siRNA and Six5 siRNA reduced Six1, Six4 and Six5 protein levels to around 25%, 25% and 40%, respectively, compared to the negative control, when assayed 48 hours after transfection (Fig. 6A).

To investigate the roles of *Six* genes in the proliferation of muscle satellite cells, cell number was counted at 48 hours after transfection of each siRNA and compared to the number of muscle satellite cells transfected with negative control siRNA (Fig. 6B). Six1 siRNA and Six4 siRNA did not significantly change the proportion of such cells (1.33 ± 0.56 and 0.87 ± 0.12-fold, respectively). In contrast, transfection of Six5 siRNA robustly increased the ratio to 5.4 ± 0.71-fold.

To analyze whether knockdown of *Six* genes altered differentiation properties of muscle satellite cells, we performed immunofluorescence of skeletal muscle myosin to assess the extent of muscle differentiation. Twelve hours after transfection of each siRNA, the medium was replaced with the differentiation medium and cells were incubated for additional 36 hours. The proportion of

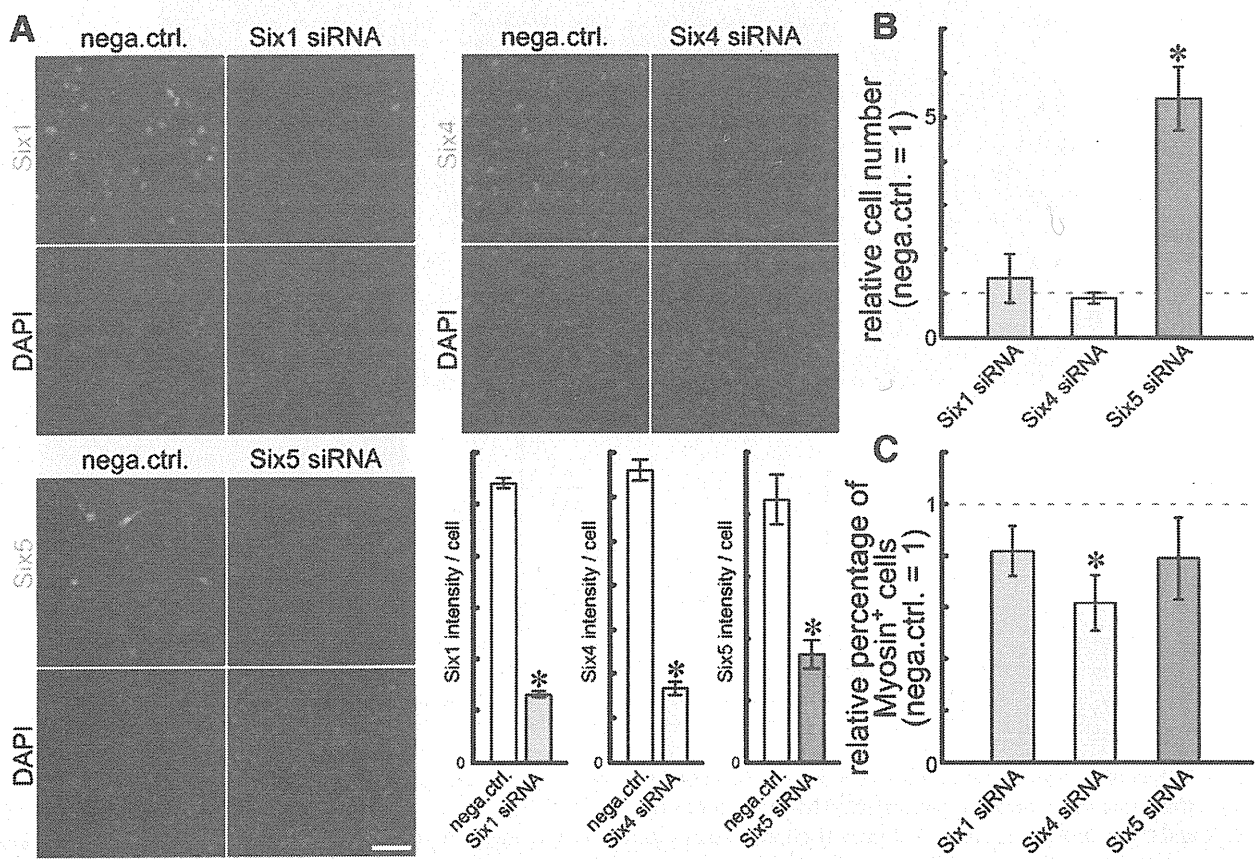

Fig. 6 – Effects of knockdown of *Six1*, *Six4* and *Six5* on proliferation and differentiation of satellite cells. (A) Immunofluorescence of satellite cells transfected with negative control siRNA, Six1 siRNA, Six4 siRNA and Six5 siRNA in growth medium using antibodies to Six1, Six4 and Six5 shown in green. Nuclei were stained with DAPI (blue). The intensity of immunofluorescence of typical result was densitometrically analyzed and displayed in bar graphs. Data are mean ± SEM. *$p < 0.01$, compared with negative control siRNA. Scale bar: 50 μm. Note no obvious increase in picnotic nuclei stained with DAPI in the siRNA-transfected cells, suggesting the marginal cytotoxicity caused by Stealth siRNA. (B) Forty-eight hours after transfection of siRNAs, the cell numbers transfected with Six1 siRNA, Six4 siRNA and Six5 siRNA were counted and normalized by that of negative control siRNA. Data are mean ± SEM of three independent cell isolates. *$p = 0.004$, compared with negative control siRNA. (C) Satellite cells were transfected with siRNAs and cultured in differentiation medium. The percentage of skeletal muscle myosin-positive cells among total cells treated with Six1 siRNA, Six4 siRNA and Six5 siRNA was determined and expressed relative to that of negative control siRNA. Data are mean ± SEM of four independent cell isolates. *$p = 0.01$, compared with the negative control siRNA.

skeletal muscle myosin-positive cells among total cells was determined and normalized by that of muscle satellite cells transfected with negative control siRNA (Fig. 6C). The relative ratios of skeletal muscle myosin-positive cells were reduced to 0.81 ± 0.10, $0.61 \pm 0.11$and 0.79 ± 0.16-fold by the transfection of Six1 siRNA, Six4 siRNA and Six5 siRNA, respectively. However, only the reduction provided by Six4 siRNA was statistically significant. These results indicate that Six5 regulates the proliferation of muscle satellite cells while Six4 plays a role in the differentiation of these cells.

Altered proliferation of muscle satellite cells in Six4$^{+/-}$Six5$^{-/-}$ mice

We further analyzed the roles of *Six* genes in the proliferation and differentiation of muscle satellite cells by characterizing these cells in *Six* gene-deficient mice. Such analysis would corroborate the data obtained from siRNA-mediated knockdown experiments. However, among the knockout mice of *Six* genes, *Six1*$^{-/-}$ mice die immediately after birth [11] and it is impossible to analyze satellite cells derived from adult skeletal muscles. Since *Six4*$^{-/-}$ and *Six5*$^{-/-}$ mice are viable and do not show apparent muscle phenotypes [16,24,36] (and data not shown), we intercrossed *Six4*$^{+/-}$*Six5*$^{+/-}$ mice to obtain adult with the smallest dosage of *Six* genes. All *Six4*$^{-/-}$*Six5*$^{-/-}$ mice were never born and *Six4*$^{-/-}$*Six5*$^{+/-}$ mice were rarely born in less than Mendelian ratio (data not shown). On the other hand, *Six4*$^{+/-}$*Six5*$^{-/-}$ mice were viable and did not show obvious phenotype in adult skeletal muscles (data not shown). Thus, we were able to evaluate the behavior of satellite cells with the smallest dosage of *Six* genes in *Six4*$^{+/-}$*Six5*$^{-/-}$ mice.

SM/C-2.6-positive cells were isolated from limb and back muscles of 8- to 12-week-old *Six4*$^{+/-}$*Six5*$^{-/-}$ mice and their proliferation and differentiation were compared with those of age-matched wild-type mice (Fig. 7). The total number of muscle satellite cells isolated from *Six4*$^{+/-}$*Six5*$^{-/-}$ mice was not significantly different from those of wild-type mice (data not shown). The isolated satellite cells were plated at two different densities, 6.5×10^3 and 1.3×10^4 cells/cm^2 (Fig. 7A plating) and cultured in the growth medium. The cells were harvested and counted every day for 4 days after plating. One day after plating at low density (6.5×10^3 cells/cm^2), the cell density of satellite cells from *Six4*$^{+/-}$*Six5*$^{-/-}$ mice was significantly higher than that from wild-type mice (Fig. 7A day 1, solid circles). From day 1 to day 4, the density of satellite cells from *Six4*$^{+/-}$*Six5*$^{-/-}$ was consistently higher than that from wild-type (Fig. 7A day 1–day 4, solid circles). When the culture contained a higher density of these cells (1.3×10^4 cells/cm^2), the density of satellite cells from *Six4*$^{+/-}$*Six5*$^{-/-}$ was also consistently higher than that from wild-type after plating (Fig. 7A day 1–day 4, solid squares). Although the satellite cells derived from both genotypes reached a proliferation plateau at 3 days after plating, the cell density at the plateau was also higher in the *Six4*$^{+/-}$*Six5*$^{-/-}$ mice than in wild-type mice (Fig. 7A day 3–day 4, solid squares). Considered together, these results suggest that satellite cells from *Six4*$^{+/-}$*Six5*$^{-/-}$ begin proliferation earlier and grow to a higher cell density, compared to wild-type satellite cells. The possibilities that the observed differences were due to the plating efficiency of the cells or recovery from passage were not excluded.

To analyze whether muscle satellite cells from *Six4*$^{+/-}$*Six5*$^{-/-}$ mice have altered differentiation properties, the satellite cells from wild-type and *Six4*$^{+/-}$*Six5*$^{-/-}$ mice were cultured in the differentiation medium at two different densities, 2×10^4 and 4×10^4 cells/cm^2. We performed immunofluorescence of skeletal muscle myosin to estimate the extent of muscle differentiation. At plating

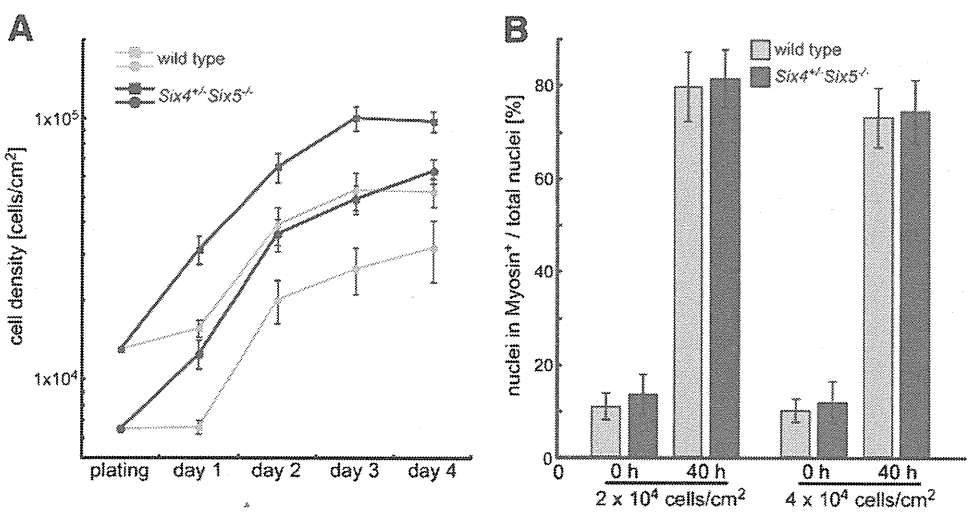

Fig. 7 – Proliferation of muscle satellite cells from *Six4*$^{+/-}$*Six5*$^{-/-}$ and wild-type mice. (A) Isolated satellite cells were plated at two different densities, 6.5×10^3 (circles) and 1.3×10^4 (squares) cells/cm^2. After plating, the cell densities of satellite cells from the wild-type (gray symbols) and *Six4*$^{+/-}$*Six5*$^{-/-}$ (black symbols) mice were calculated at 1 day (day 1), 2 days (day 2), 3 days (day 3) and 4 days (day 4) in the growth medium. Data are mean ± SEM of three independent cell isolates. (B) Satellite cells from wild-type (gray bars) and *Six4*$^{+/-}$*Six5*$^{-/-}$ (black bars) mice were plated at two different densities, 2×10^4 (left side) and 4×10^4 (right side) cells/cm^2. Two hours later, the culture medium was replaced with the differentiation medium to induce differentiation of myotubes. The percentage of nuclei of the satellite cells positive for skeletal muscle myosin immunofluorescence was calculated at medium change to differentiation medium (0 h) and 40 hours after medium change (40 h). Data are mean ± SEM of four independent cell isolates.

(one passage after preparation), the percentage of satellite cells expressing skeletal muscle myosin was not significantly different between wild-type and *Six4*$^{+/-}$*Six5*$^{-/-}$ (data not shown). Two hours after plating, the medium was replaced with the differentiation medium. Satellite cells were collected at 0 and 40 hours after the medium change. At 0 hour, the percentages of skeletal muscle myosin-positive satellite cells were similar in the wild-type (10.7 ± 2.79%) and *Six4*$^{+/-}$*Six5*$^{-/-}$(13.4 ± 4.29%), when plated at low cell density (2×10^4 cells/cm^2) (Fig. 7B 0 h). At 40 hours after the medium change, the percentage of skeletal muscle myosin-positive cells in wild-type (79.5 ± 7.51%) was similar to that in *Six4*$^{+/-}$*Six5*$^{-/-}$ (81.2 ± 6.30%, Fig. 7B 40 h). Even when satellite cells were plated at high density (4×10^4 cells/cm^2), the percentages of skeletal muscle myosin-positive cells in the wild-type were not significantly different from *Six4*$^{+/-}$*Six5*$^{-/-}$ at 0 and 40 hours (9.91 ± 2.57 and 11.7 ± 4.49% at 0 hour, 73.0 ± 6.34 and 74.3 ± 6.73% at 40 hours, respectively). These results suggest that the differentiation capacity of *Six4*$^{+/-}$*Six5*$^{-/-}$ satellite cells is similar to that of the wild-type. Considered together, the analysis of satellite cells from *Six4*$^{+/-}$*Six5*$^{-/-}$ mice indicates that either *Six4* or *Six5* or both play a role in the regulation of muscle satellite cell proliferation.

Discussion

Muscle satellite cells are one of the most important players in muscle regeneration. Understanding the control mechanisms of their proliferation and differentiation is important for the development of cell-based therapy for muscle disorders such as dystrophy using these cells [37]. The roles of the members of *Six* family genes, especially *Six1*, *Six4* and *Six5*, have been extensively studied during embryonic development of skeletal muscle and the results indicate that they play critical roles in myogenesis [21–23]. However, the involvement of these genes in muscle regeneration and behavior of satellite cells has never been addressed. This study demonstrated, for the first time, the roles of *Six* family genes in muscle satellite cells.

Robust induction of Six1- and Six4-positive cells was observed in regenerating muscle three days after damage by cardiotoxin injection in adult skeletal muscle (Fig. 1). Many of these cells were also positive for MyoD, which is known to be expressed in myoblasts produced rapidly during regeneration, and mitotic marker Ki67. Thus, these cells are considered to be myogenic precursor cells. The quiescent muscle satellite cells marked by Pax7 and M-cadherin in the myofibers were also positive for Six1 and Six4 (Fig. 2). In addition, the muscle satellite cells isolated by SM/C-2.6 antibody are positive for Six1, Six4 and Six5 under proliferation and differentiation conditions (Fig. 2). These observations prompted us to investigate in detail the roles of Six1, Six4 and Six5 in the proliferation and differentiation of muscle satellite cells.

One of the intriguing findings of our study is that *Six* genes were involved in the control of cell proliferation of muscle satellite cells. Overexpression of *Six1*, *Six4* or *Six5* in isolated muscle satellite cells inhibited the proliferation as observed by a reduction in the number of cells positive for phospho-histone H3 and Ki67 (Fig. 3). Conversely, siRNA-mediated knockdown of *Six5* resulted in a robust increase in cell number (Fig. 6). These results mean that the proliferation of muscle satellite cells is negatively regulated when the amount of Six proteins exceeds the normal level, while it is normally repressed by Six5 protein present in the cells. These findings highlight the primary repressive role of Six5 in proliferation of activated satellite cells. Moreover, muscle satellite cells from *Six4*$^{+/-}$*Six5*$^{-/-}$ mice proliferated to higher cell density (Fig. 7), consistent with the role of *Six5* defined in overexpression and knockdown experiments. Because we observed the proliferation of isolated satellite cells, the effect of decreased gene dosage of *Six4* and *Six5* is not through altered niche but is rather cell-autonomous change within the satellite cells. Since inactivation of p16^{INK4a}/cyclinD1/Rb pathway is reported to cause rapid and prolonged mitogenic stimulation [38,39], which is reminiscent of the satellite cells from *Six4*$^{+/-}$*Six5*$^{-/-}$ mice, further analysis of the contribution of Six proteins to the regulatory components of cell cycle is required. Reducing the amount of Six5 protein in muscle satellite cells lead to efficient amplification of the cells without changing the differentiation properties (Fig. 6). This remarkable finding suggests that Six5 may be a good candidate as a molecular target in terms of satellite cell therapy. The amount of Six proteins is maintained at critical level for the normal proliferation of satellite cells. Moreover, variable amount and subcellular localization of each of the Six proteins in individual satellite cells might correlate with their function on proliferation and differentiation (Figs. 1 and 2). These aspects of the Six proteins need to be elucidated in the future.

Six1$^{-/-}$ mice show low cell proliferation capacity in the mouse otic vesicle [11,12]. Overexpression of *Xenopus Optix2*, one of the members of *Xenopus Six* family genes, causes retinal field enlargement due to the augmented proliferation [40]. Six proteins influence the cell cycle by regulating the expression of cyclinA1 [41], c-Myc and cyclinD1 [42,43]. These observations implicate a positive regulatory role for Six proteins in cell proliferation. In sharp contrast, Six proteins repress cell proliferation in muscle satellite cells. This may be related to the function of Six1 in stimulating the differentiation of muscle satellite cells or to cell types that provide different context to Six proteins in terms of their functions.

Another interesting finding is the differential role of Six1 and Six4/Six5 in the control of differentiation of muscle satellite cells. Overproduction of Six1 stimulated muscle differentiation estimated by the fusion index and mean number of nuclei in skeletal muscle myosin-positive cells (Fig. 4). In contrast, overexpression of *Six4* and *Six5* inhibited cell differentiation. The main reason for the differential control of cell differentiation might be related to the differential effects of these Six proteins on the expression of myogenin. In cultured cell transfection assays, Six1, Six2, Six4 and Six5 similarly activated the *myogenin* promoter activity in conjunction with Eya coactivator [26,27]. Similarly, *in vivo*, Six1 and Six4 also activated *myogenin* promoter [26]. In isolated muscle satellite cells, overproduction of Six1 activated the expression of myogenin. In sharp contrast, overproduction of Six4 and Six5 greatly reduced the expression of myogenin (Fig. 5). Thus, Six1 might be the primary Six protein that activates *myogenin* promoter in satellite cells. Indeed, Six1 is known to be required for the proper activation of myogenin in limb muscle development [15]. Moreover, the recent finding of Ski pro-oncogene promotion of C2C12 myoblast differentiation through transcriptional activation of *myogenin* in a complex with Six1 and Eya3 is consistent with this notion [44]. The precise molecular basis for the abovementioned differential effects of Six family proteins on the myogenin

expression is unknown. While it is possible that Six4 and Six5 destabilize the myogenin protein, it is more plausible that the differential effect on myogenin expression is at a transcriptional level. Interestingly, we found a profound reduction in Six1 protein level in the satellite cells upon overexpression of Six4 and Six5 (Supplementary Fig. 3). This suggests the indirect repression mechanisms of myogenin by Six4 and Six5. In this context, the recent report that described the binding of Six1 to the regulatory region of *Six1*, *Six4* and *Six5* [45] supports this notion. Because Six1 shares the binding consensus with Six4 and Six5 [46,47], the possible cross-regulations among *Six* genes has been proposed [45]. On the other hand, Six4 and Six5 may be involved in the direct repression of *myogenin* promoter instead of Six1 that activates the promoter. Considering that Six1 and Six4/Six5 had opposite effects on *myogenin* promoter, it should be noted that Six1 and Six4/Six5 each has a distinct molecular structure. The latter two members have a large C-terminal portion in addition to the conserved Six domain and homeodomain [8,48]. This portion may be involved in the differential function of each Six family protein. If this is the case, it is not surprising that Six1 and Six4/Six5 display differential regulatory role in muscle differentiation.

Because *Six* family genes can modulate the proliferation and differentiation of muscle satellite cells, it is tempting to alter the dosage *Six* genes and analyze their effects on muscle regeneration *in vivo*. We are currently addressing the roles of Six family proteins by examining muscle regeneration in *mdx* mice, in which muscle regeneration occurs more frequently in adults. We are crossing *mdx* mice and defective mice harboring lower gene dosage of *Six* or higher dosage of *Six1*. This approach should uncover the physiological roles of *Six* family genes in the regeneration of skeletal muscles.

Materials and methods

Animals

C57BL/6 mice were purchased from Nihon CLEA (Tokyo, Japan). $Six4^{+/-}$ mice were generated as described previously [16]. $Six5^{+/-}$ mice were generously provided by Dr. S. J. Tapscott [24] and crossed with $Six4^{+/-}$ mice to obtain $Six4^{+/-}Six5^{+/-}$ mice. The intercrosses of $Six4^{+/-}Six5^{+/-}$ mice yielded $Six4^{+/-}Six5^{-/-}$ mice. PCR or Southern blotting was performed to verify the genotypes of offspring as described previously [16,24]. Mice were housed in an environmentally controlled room in the Center for Experimental Medicine of Jichi Medical University, under the guidelines for animal experiments. All experimental protocols were approved by the Ethics Review Committee for Animal Experimentation of Jichi Medical University.

Injection of cardiotoxin

To induce muscle regeneration, cardiotoxin (10 μmol/L 5 μl/body weight (g); Sigma, St. Louis, MO) was injected into the TA muscles of 8- to 12-week-old C57BL/6 mice. Three days after injection, TA muscles were harvested and processed for immunofluorescence.

Immunofluorescence

TA muscles were fixed in 4% paraformaldehyde/phosphate-buffered saline (PBS) for 2 hours at 4 °C. Samples were incubated in 30% sucrose/PBS and then embedded in optimal cutting temperature (OCT) compound (Sakura Finetek, Torrance, CA) for freezing and cryosectioning (10–12 μm in thickness). Cultured cells were fixed with 4% paraformaldehyde/PBS for 10 minutes. The following primary antibodies were used in immunofluorescence: guinea pig anti-Six1 antibody (1:5000 dilution [18]), rat anti-Six1 antibody (1:2000 dilution [10]), guinea pig anti-Six4 antibody (1:2000 dilution, [10]), affinity-purified rabbit anti-Six5 antibody (1:500 dilution, [49]), rabbit anti-laminin antibody (1:1500 dilution, Sigma), rabbit anti-MyoD antibody (1:500 dilution, Santa Cruz Biotechnology, Santa Cruz, CA), mouse anti-Pax7 antibody (hybridoma supernatant, Developmental Studies Hybridoma Bank), rabbit anti-M-cadherin antibody (1:1000 dilution, [50]), mouse anti-skeletal muscle myosin antibody (MY-32) (1:30 dilution, Zymed, San Francisco, CA), rabbit anti-phospho-histone H3 (Ser10) antibody (1:1000 dilution, Millipore, Billerica, MA), rabbit anti-Ki67 antibody (1:30 dilution, YLEM, Italy) and mouse anti-myogenin antibody (F5D) (1:500 dilution, Santa Cruz Biotechnology). For anti-Pax7 antibody, M.O.M. Mouse Ig Blocking Reagent (Vector Laboratories, Burlingame, CA) was used to eliminate the background from endogenous mouse immunoglobulins. To visualize the immunoreactions of primary antibodies, fluorescent-labeled secondary antibodies were used at 1:2000 dilution as follows: anti-rabbit conjugated Cy5 (Amersham Biosciences, Piscataway, NJ), Alexa Fluor 488 anti-rabbit, Alexa Fluor 488 anti-rat, Alexa Fluor 488 anti-guinea pig, Alexa Fluor 546 anti-mouse, Alexa Fluor 546 anti-rabbit, Alexa Fluor 546 anti-rat, Alexa Fluor 546 anti-guinea pig and Alexa Fluor 633 anti-mouse (Molecular Probes/Invitrogen, Carlsbad, CA). 4′6-Diamidino-2-phenylindole (DAPI, Sigma) was used at 50 ng/ml to stain nuclei. The immunofluorescent images were captured with Olympus FV1000 confocal microscope and electronically assigned to red, green or blue channels (Olympus Optical, Tokyo, Japan).

Isolation of satellite cells

Muscle satellite cells were isolated from limb and back muscles of 8- to 12-week-old C57BL/6 or $Six4^{+/-}Six5^{-/-}$ mice by using SM/C-2.6 monoclonal antibody as described previously [4,5]. The sorted cells were expanded on Matrigel (BD, Franklin Lakes, NJ)-coated dishes in a growth medium, DMEM, containing 20% fetal bovine serum, human recombinant bFGF (2.5 ng/ml) (Invitrogen), recombinant mouse HGF (25 ng/ml) (R&D Systems) and heparin (5 μg/ml) (Sigma). To induce differentiation of the satellite cells, the growth medium was replaced with differentiation medium (2% horse serum/DMEM). The culture medium was replaced with a fresh medium every day. Satellite cells derived from EDL were prepared and cultured as described previously [51] and used for siRNA experiments.

Retrovirus vectors and infection

Flag-tagged mouse *Six1*, *Six4* and *Six5* cDNAs [27,52] were cloned into the multiple cloning site upstream of IRES-EGFP of pMXs-IG vector, which was kindly provided by Dr. T. Kitamura [33]. Retroviral particles were produced by transfection of vector plasmids into PLAT-E packaging cells as described previously [33,53]. Muscle satellite cells were plated at 1.3×10^4 cells/cm^2 in growth medium one passage after the preparation. The next day, the medium was replaced with growth medium containing retroviral particles. Two days after infection, the culture medium

was replaced with growth medium or differentiation medium and the cells were incubated for 24 hours for the assays under proliferating condition or differentiation condition, respectively.

Western blotting

Nuclear and cytoplasmic extracts of proliferating muscle satellite cells isolated from 8-week-old *Six4*$^{-/-}$ mice and C2C12 cells were prepared and analyzed by western blotting using anti-Six5 antibody [49] as described previously [27,54].

Fusion index and statistics

Fusion index was calculated as [(number of nuclei in EGFP-positive myotubes (>2 myonuclei) / total nuclei within EGFP-positive cells) × 100%] [55–57]. Differences from the control experiments were tested statistically by the Student's *t*-test. All values are expressed as mean ± SEM. A probability of less than 5% was considered statistically significant.

RNA interference

The Stealth RNAi siRNA Negative Control Med GC Duplex and Stealth Select siRNAs targeted to mouse *Six1*, *Six4* and *Six5* were purchased from Invitrogen (Carlsbad, CA). Six1 siRNA is a mixture of equimolar amounts of Six1-MSS237917, Six1-MSS237918 and Six1-MSS237919. Six4 siRNA consists of Six4-MSS209042, Six4-MSS209043 and Six4-MSS209044. Six5 siRNA consists of Six5-MSS277077, Six5-MSS277078 and Six5-MSS277079. Sequences for each siRNA species were provided by the company under license. The transfection of Stealth siRNA into satellite cells isolated from EDL was performed using Lipofectamine RNAiMAX (Invitrogen) as described previously [51] with slight modifications.

Supplementary materials related to this article can be found online at doi:10.1016/j.yexcr.2010.08.001.

Acknowledgments

We thank Stephen J. Tapscott for *Six5*$^{-/-}$ mice and reading the manuscript and Toshio Kitamura for pMXs-IG plasmid and PLAT-E cell. We are grateful to So-ichiro Fukada for providing SM/C-2.6 antibody and for the helpful discussion. We also thank Hiroko Ikeda, Yuki Takano, Kanako Mogi, Yuko Suto and Miho Akima for the excellent technical assistance. This work was supported by Research Grant No. 17A-10 for Nervous and Mental Disorders from the Ministry of Health, Labour and Welfare, Intramural Research Grant No. 20B-13 for Neurological and Psychiatric Disorders of NCNP, Support Program for Scientific Research Platform in Private Universities (SPSRP) to JMU and a grant from The Nakatomi Foundation.

REFERENCES

[1] A. Mauro, Satellite cell of skeletal muscle fibers, J. Biophys. Biochem. Cytol. 9 (1961) 493–495.
[2] A. Otto, H. Collins-Hooper, K. Patel, The origin, molecular regulation and therapeutic potential of myogenic stem cell populations, J. Anat. 215 (2009) 477–497.
[3] P.S. Zammit, J.P. Golding, Y. Nagata, V. Hudon, T.A. Partridge, J.R. Beauchamp, Muscle satellite cells adopt divergent fates: a mechanism for self-renewal? J. Cell Biol. 166 (2004) 347–357.
[4] S. Fukada, S. Higuchi, M. Segawa, K. Koda, Y. Yamamoto, K. Tsujikawa, Y. Kohama, A. Uezumi, M. Imamura, Y. Miyagoe-Suzuki, S. Takeda, H. Yamamoto, Purification and cell-surface marker characterization of quiescent satellite cells from murine skeletal muscle by a novel monoclonal antibody, Exp. Cell Res. 296 (2004) 245–255.
[5] S. Fukada, A. Uezumi, M. Ikemoto, S. Masuda, M. Segawa, N. Tanimura, H. Yamamoto, Y. Miyagoe-Suzuki, S. Takeda, Molecular signature of quiescent satellite cells in adult skeletal muscle, Stem Cells 25 (2007) 2448–2459.
[6] M.A. Serikaku, J.E. O'Tousa, sine oculis is a homeobox gene required for Drosophila visual system development, Genetics 138 (1994) 1137–1150.
[7] B.N. Cheyette, P.J. Green, K. Martin, H. Garren, V. Hartenstein, S.L. Zipursky, The Drosophila sine oculis locus encodes a homeodomain-containing protein required for the development of the entire visual system, Neuron 12 (1994) 977–996.
[8] K. Kawakami, S. Sato, H. Ozaki, K. Ikeda, Six family genes—structure and function as transcription factors and their roles in development, Bioessays 22 (2000) 616–626.
[9] H. Kobayashi, K. Kawakami, M. Asashima, R. Nishinakamura, Six1 and Six4 are essential for Gdnf expression in the metanephric mesenchyme and ureteric bud formation, while Six1 deficiency alone causes mesonephric-tubule defects, Mech. Dev. 124 (2007) 290–303.
[10] Y. Konishi, K. Ikeda, Y. Iwakura, K. Kawakami, Six1 and Six4 promote survival of sensory neurons during early trigeminal gangliogenesis, Brain Res. 1116 (2006) 93–102.
[11] H. Ozaki, K. Nakamura, J. Funahashi, K. Ikeda, G. Yamada, H. Tokano, H.O. Okamura, K. Kitamura, S. Muto, H. Kotaki, K. Sudo, R. Horai, Y. Iwakura, K. Kawakami, Six1 controls patterning of the mouse otic vesicle, Development 131 (2004) 551–562.
[12] W. Zheng, L. Huang, Z.B. Wei, D. Silvius, B. Tang, P.X. Xu, The role of Six1 in mammalian auditory system development, Development 130 (2003) 3989–4000.
[13] P.X. Xu, W. Zheng, L. Huang, P. Maire, C. Laclef, D. Silvius, Six1 is required for the early organogenesis of mammalian kidney, Development 130 (2003) 3085–3094.
[14] C. Laclef, E. Souil, J. Demignon, P. Maire, Thymus, kidney and craniofacial abnormalities in Six 1 deficient mice, Mech. Dev. 120 (2003) 669–679.
[15] C. Laclef, G. Hamard, J. Demignon, E. Souil, C. Houbron, P. Maire, Altered myogenesis in Six1-deficient mice, Development 130 (2003) 2239–2252.
[16] H. Ozaki, Y. Watanabe, K. Takahashi, K. Kitamura, A. Tanaka, K. Urase, T. Momoi, K. Sudo, J. Sakagami, M. Asano, Y. Iwakura, K. Kawakami, Six4, a putative myogenin gene regulator, is not essential for mouse embryonal development, Mol. Cell. Biol. 21 (2001) 3343–3350.
[17] G. Oliver, R. Wehr, N.A. Jenkins, N.G. Copeland, B.N. Cheyette, V. Hartenstein, S.L. Zipursky, P. Gruss, Homeobox genes and connective tissue patterning, Development 121 (1995) 693–705.
[18] K. Ikeda, S. Ookawara, S. Sato, Z. Ando, R. Kageyama, K. Kawakami, Six1 is essential for early neurogenesis in the development of olfactory epithelium, Dev. Biol. 311 (2007) 53–68.
[19] Y. Suzuki, K. Ikeda, K. Kawakami, Regulatory role of Six1 in the development of taste papillae, Cell Tissue Res. 339 (2010) 513–525.
[20] K. Ikeda, R. Kageyama, Y. Suzuki, K. Kawakami, Six1 is indispensable for production of functional apical and basal progenitors during olfactory epithelial development, Int. J. Dev. Biol. (in press), doi:10.1387/ijdb.093041ki.
[21] R. Grifone, J. Demignon, C. Houbron, E. Souil, C. Niro, M.J. Seller, G. Hamard, P. Maire, Six1 and Six4 homeoproteins are required for Pax3 and Mrf expression during myogenesis in the mouse embryo, Development 132 (2005) 2235–2249.

[22] R. Grifone, C. Laclef, F. Spitz, S. Lopez, J. Demignon, J.E. Guidotti, K. Kawakami, P.X. Xu, R. Kelly, B.J. Petrof, D. Daegelen, J.P. Concordet, P. Maire, Six1 and Eya1 expression can reprogram adult muscle from the slow-twitch phenotype into the fast-twitch phenotype, Mol. Cell. Biol. 24 (2004) 6253–6267.
[23] C. Niro, J. Demignon, S. Vincent, Y. Liu, J. Giordani, N. Sgarioto, M. Favier, I. Guillet-Deniau, A. Blais, P. Maire, Six1 and Six4 gene expression is necessary to activate the fast-type muscle gene program in the mouse primary myotome, Dev. Biol. 338 (2010) 168–182.
[24] T.R. Klesert, D.H. Cho, J.I. Clark, J. Maylie, J. Adelman, L. Snider, E.C. Yuen, P. Soriano, S.J. Tapscott, Mice deficient in Six5 develop cataracts: implications for myotonic dystrophy, Nat. Genet. 25 (2000) 105–109.
[25] S.K. Heath, S. Carne, C. Hoyle, K.J. Johnson, D.J. Wells, Characterisation of expression of mDMAHP, a homeodomain-encoding gene at the murine DM locus, Hum. Mol. Genet. 6 (1997) 651–657.
[26] F. Spitz, J. Demignon, A. Porteu, A. Kahn, J.P. Concordet, D. Daegelen, P. Maire, Expression of myogenin during embryogenesis is controlled by Six/sine oculis homeoproteins through a conserved MEF3 binding site, Proc. Natl. Acad. Sci. U. S. A. 95 (1998) 14220–14225.
[27] H. Ohto, S. Kamada, K. Tago, S.I. Tominaga, H. Ozaki, S. Sato, K. Kawakami, Cooperation of six and eya in activation of their target genes through nuclear translocation of Eya, Mol. Cell. Biol. 19 (1999) 6815–6824.
[28] E.N. Olson, W.H. Klein, bHLH factors in muscle development: dead lines and commitments, what to leave in and what to leave out, Genes Dev. 8 (1994) 1–8.
[29] K. Yun, B. Wold, Skeletal muscle determination and differentiation: story of a core regulatory network and its context, Curr. Opin. Cell Biol. 8 (1996) 877–889.
[30] D.D. Cornelison, B.J. Wold, Single-cell analysis of regulatory gene expression in quiescent and activated mouse skeletal muscle satellite cells, Dev. Biol. 191 (1997) 270–283.
[31] P. Seale, L.A. Sabourin, A. Girgis-Gabardo, A. Mansouri, P. Gruss, M.A. Rudnicki, Pax7 is required for the specification of myogenic satellite cells, Cell 102 (2000) 777–786.
[32] A. Irintchev, M. Zeschnigk, A. Starzinski-Powitz, A. Wernig, Expression pattern of M-cadherin in normal, denervated, and regenerating mouse muscles, Dev. Dyn. 199 (1994) 326–337.
[33] T. Kitamura, Y. Koshino, F. Shibata, T. Oki, H. Nakajima, T. Nosaka, H. Kumagai, Retrovirus-mediated gene transfer and expression cloning: powerful tools in functional genomics, Exp. Hematol. 31 (2003) 1007–1014.
[34] Y. Nabeshima, K. Hanaoka, M. Hayasaka, E. Esumi, S. Li, I. Nonaka, Myogenin gene disruption results in perinatal lethality because of severe muscle defect, Nature 364 (1993) 532–535.
[35] P. Hasty, A. Bradley, J.H. Morris, D.G. Edmondson, J.M. Venuti, E.N. Olson, W.H. Klein, Muscle deficiency and neonatal death in mice with a targeted mutation in the myogenin gene, Nature 364 (1993) 501–506.
[36] P.S. Sarkar, B. Appukuttan, J. Han, Y. Ito, C. Ai, W. Tsai, Y. Chai, J.T. Stout, S. Reddy, Heterozygous loss of Six5 in mice is sufficient to cause ocular cataracts, Nat. Genet. 25 (2000) 110–114.
[37] M.A. Rudnicki, F. Le Grand, I. McKinnell, S. Kuang, The molecular regulation of muscle stem cell function, Cold Spring Harb. Symp. Quant. Biol. 73 (2008) 323–331.
[38] M. Serrano, H. Lee, L. Chin, C. Cordon-Cardo, D. Beach, R.A. DePinho, Role of the INK4a locus in tumor suppression and cell mortality, Cell 85 (1996) 27–37.
[39] J.L. Dean, A.K. McClendon, K.R. Stengel, E.S. Knudsen, Modeling the effect of the RB tumor suppressor on disease progression: dependence on oncogene network and cellular context, Oncogene 29 (2010) 68–80.
[40] M.E. Zuber, M. Perron, A. Philpott, A. Bang, W.A. Harris, Giant eyes in Xenopus laevis by overexpression of XOptx2, Cell 98 (1999) 341–352.
[41] R.D. Coletta, K. Christensen, K.J. Reichenberger, J. Lamb, D. Micomonaco, L. Huang, D.M. Wolf, C. Muller-Tidow, T.R. Golub, K. Kawakami, H.L. Ford, The Six1 homeoprotein stimulates tumorigenesis by reactivation of cyclin A1, Proc. Natl. Acad. Sci. U. S. A. 101 (2004) 6478–6483.
[42] Y. Yu, E. Davicioni, T.J. Triche, G. Merlino, The homeoprotein six1 transcriptionally activates multiple protumorigenic genes but requires ezrin to promote metastasis, Cancer Res. 66 (2006) 1982–1989.
[43] X. Li, K.A. Oghi, J. Zhang, A. Krones, K.T. Bush, C.K. Glass, S.K. Nigam, A.K. Aggarwal, R. Maas, D.W. Rose, M.G. Rosenfeld, Eya protein phosphatase activity regulates Six1-Dach-Eya transcriptional effects in mammalian organogenesis, Nature 426 (2003) 247–254.
[44] H. Zhang, E. Stavnezer, Ski regulates muscle terminal differentiation by transcriptional activation of Myog in a complex with Six1 and Eya3, J. Biol. Chem. 284 (2009) 2867–2879.
[45] Y. Liu, A. Chu, I. Chakroun, U. Islam, A. Blais, Cooperation between myogenic regulatory factors and SIX family transcription factors is important for myoblast differentiation, Nucleic Acids Res. (in press), doi:10.1093/nar/gkq585.
[46] Z. Ando, S. Sato, K. Ikeda, K. Kawakami, Slc12a2 is a direct target of two closely related homeobox proteins, Six1 and Six4, FEBS J. 272 (2005) 3026–3041.
[47] S. Sato, M. Nakamura, D.H. Cho, S.J. Tapscott, H. Ozaki, K. Kawakami, Identification of transcriptional targets for Six5: implication for the pathogenesis of myotonic dystrophy type 1, Hum. Mol. Genet. 11 (2002) 1045–1058.
[48] K. Kawakami, H. Ohto, K. Ikeda, R.G. Roeder, Structure, function and expression of a murine homeobox protein AREC3, a homologue of Drosophila sine oculis gene product, and implication in development, Nucleic Acids Res. 24 (1996) 303–310.
[49] H. Ohto, T. Takizawa, T. Saito, M. Kobayashi, K. Ikeda, K. Kawakami, Tissue and developmental distribution of Six family gene products, Int. J. Dev. Biol. 42 (1998) 141–148.
[50] K. Ojima, A. Uezumi, H. Miyoshi, S. Masuda, Y. Morita, A. Fukase, A. Hattori, H. Nakauchi, Y. Miyagoe-Suzuki, S. Takeda, Mac-1(low) early myeloid cells in the bone marrow-derived SP fraction migrate into injured skeletal muscle and participate in muscle regeneration, Biochem. Biophys. Res. Commun. 321 (2004) 1050–1061.
[51] Y. Ono, V.F. Gnocchi, P.S. Zammit, R. Nagatomi, Presenilin-1 acts via Id1 to regulate the function of muscle satellite cells in a gamma-secretase-independent manner, J. Cell Sci. 122 (2009) 4427–4438.
[52] H. Ozaki, Y. Watanabe, K. Ikeda, K. Kawakami, Impaired interactions between mouse Eya1 harboring mutations found in patients with branchio-oto-renal syndrome and Six, Dach, and G proteins, J. Hum. Genet. 47 (2002) 107–116.
[53] S. Morita, T. Kojima, T. Kitamura, Plat-E: an efficient and stable system for transient packaging of retroviruses, Gene Ther. 7 (2000) 1063–1066.
[54] K. Kawakami, K. Yanagisawa, Y. Watanabe, S. Tominaga, K. Nagano, Different factors bind to the regulatory region of the Na+, K(+)-ATPase alpha 1-subunit gene during the cell cycle, FEBS Lett. 335 (1993) 251–254.
[55] V. Jacquemin, D. Furling, A. Bigot, G.S. Butler-Browne, V. Mouly, IGF-1 induces human myotube hypertrophy by increasing cell recruitment, Exp. Cell Res. 299 (2004) 148–158.
[56] V. Horsley, K.M. Jansen, S.T. Mills, G.K. Pavlath, IL-4 acts as a myoblast recruitment factor during mammalian muscle growth, Cell 113 (2003) 483–494.
[57] V. Horsley, B.B. Friday, S. Matteson, K.M. Kegley, J. Gephart, G.K. Pavlath, Regulation of the growth of multinucleated muscle cells by an NFATC2-dependent pathway, J. Cell Biol. 153 (2001) 329–338.

The American Journal of Pathology, Vol. 176, No. 5, May 2010

DOI: 10.2353/ajpath.2010.090887

Musculoskeletal Pathology

Genetic Background Affects Properties of Satellite Cells and *mdx* Phenotypes

So-ichiro Fukada,* Daisuke Morikawa,* Yukiko Yamamoto,* Tokuyuki Yoshida,* Noriaki Sumie,* Masahiko Yamaguchi,* Takahito Ito,* Yuko Miyagoe-Suzuki,† Shin'ichi Takeda,† Kazutake Tsujikawa,* and Hiroshi Yamamoto*

From the Department of Immunology, Graduate School of Pharmaceutical Sciences, Osaka University, Osaka; and the Department of Molecular Therapy,† National Institute of Neuroscience, National Center of Neurology and Psychiatry, Tokyo, Japan*

Duchenne muscular dystrophy (DMD) is the most common lethal genetic disorder of children. The *mdx* (C57BL/10 background, C57BL/10-*mdx*) mouse is a widely used model of DMD, but the histopathological hallmarks of DMD, such as the smaller number of myofibers, accumulation of fat and fibrosis, and insufficient regeneration of myofibers, are not observed in adult C57BL/10-*mdx* except for in the diaphragm. In this study, we showed that DBA/2 mice exhibited decreased muscle weight, as well as lower myofiber numbers after repeated degeneration–regeneration cycles. Furthermore, the self-renewal efficiency of satellite cells of DBA/2 is lower than that of C57BL/6. Therefore, we produced a DBA/2-*mdx* strain by crossing DBA/2 and C57BL/10-*mdx*. The hind limb muscles of DBA/2-*mdx* mice exhibited lower muscle weight, fewer myofibers, and increased fat and fibrosis, in comparison with C57BL/10-*mdx*. Moreover, remarkable muscle weakness was observed in DBA/2-*mdx*. These results indicate that the DBA/2-*mdx* mouse is a more suitable model for DMD studies, and the efficient satellite cell self-renewal ability of C57BL/10-*mdx* might explain the difference in pathologies between humans and mice. ***(Am J Pathol 2010, 176:2414–2424; DOI: 10.2353/ajpath.2010.090887)***

Duchenne muscular dystrophy (DMD) is a progressive and lethal X-linked muscular disorder caused by mutations in the dystrophin gene.[1] The dystrophin gene encodes a 427-kDa cytoskeletal protein that forms the dystrophin/glycoprotein complex at the sarcolemma with α- and β-dystroglycans, α-, β-, γ-, and δ-sarcoglycans, and other molecules, and links the cytoskeleton of myofibers to the extracellular matrix in skeletal muscle.[2,3] The lack of dystrophin in the sarcolemma disturbs the assembly of the dystrophin/glycoprotein complex and causes instability of the muscle membrane, leading to muscle degeneration and myofiber loss. The histopathological hallmarks of DMD include degeneration, necrosis, accumulation of fat and fibrosis, and insufficient regeneration of myofibers accompanied by a loss of myofibers.[4] Therefore, the manifestations of DMD are considered to result from an imbalance between degeneration and regeneration.

The function and structure of dystrophin has been elucidated by studies of a variety of dystrophin-deficient animals. Among these animal models, the *mdx* mouse (the correct nomenclature is C57BL/10-*Dmd*^{mdx}), first described in1984, is the most prolific. A spontaneous mutation (*mdx*) arose in an inbred colony of C57BL/10 mice, which have a high level of serum pyruvate kinase.[5] The muscle pathology of the mice includes active fiber necrosis, cellular infiltration, a wide range of fiber sizes, and numerous centrally nucleated regenerating fibers. However, in contrast to DMD, replacement of muscle with fat and fibrosis is not prominent, and no losses of muscle fiber and muscle weight are observed in the skeletal muscle of *mdx* mice except in the diaphragm.[6,7] In contrast, most of the limb muscles of the *mdx* mouse maintain hypertrophy and increased skeletal muscle mass throughout much of their life span.[8] One reason for the difference between DMD and *mdx* is explained by the up-regulation of expression of utrophin, a homolog of dystrophin.[9,10] Another reason has been supposed to be the excellent regeneration capacity of *mdx* com-

Supported by grants-in-aid from the Japanese Ministries of Health, Labor and Welfare, and Education, Culture, Sports, Science and Technology, Sports and Culture of Japan, and the Suzuken Memorial Foundation.

S.F. and D.M. contributed equally to this work.

Accepted for publication December 22, 2009.

Address reprint requests to So-ichiro Fukada, Ph.D., Department of Immunology, Graduate School of Pharmaceutical Sciences, Osaka University, 1-6 Yamada-oka, Suita, Osaka 565-0871, Japan. E-mail: fukada@phs.osaka-u.ac.jp.

pared with DMD. However, this hypothesis has not been verified.

Regeneration of skeletal muscle depends on the competence of muscle satellite cells. Muscle satellite cells, which account for 2 to 5% of the total nuclei in adult skeletal muscle, play a major role in muscle regeneration.[11] Under normal conditions, satellite cells are found external to the myofiber plasma membrane and beneath the muscle basal lamina,[12] and they are mitotically quiescent in adult skeletal muscle.[13] When activated by muscle damage, satellite cells proliferate, differentiate, fuse with each other or injured myofibers, and eventually regenerate mature myofibers. During the regenerative processes, satellite cells not only produce large amounts of muscle, but also renew themselves to maintain their own population.[14] In fact, it is reported that the satellite cell pool of C57BL/10 continues to respond efficiently even when the skeletal muscle is subjected to as many as 50 cycles of severe damage.[15] Therefore, it is thought that maintenance of the satellite cell pool is indispensable to retain the long-term regenerative potential for skeletal muscle injury, including in muscular dystrophies.

To investigate genetic differences in long-term regeneration potential, we first induced repeated degeneration–regeneration cycles in four inbred strains of mice. Among these strains, C57BL/6, a widely used strain akin to C57BL/10, was tolerant of repeated injury. This is consistent with the results of C57BL/10 previously described.[15] In contrast, among four inbred strains, DBA/2 mice exhibited the most remarkable skeletal muscle loss and impaired regeneration after repeated injury. Importantly, the self-renewal potential of DBA/2 satellite cells was significantly lower than that of C57BL/6. In addition, *in vitro* colony formation and proliferation assays indicated that intrinsic difference between C57BL/6 and DBA/2 satellite cells exist. Finally, we crossed the *mdx* genotype with the DBA/2 for more than five generations. At the fifth backcross, the mice are not yet fully congenic (D2.B10-*DMD*^{mdx}), and thus we refer to them as DBA/2-*mdx* hereafter. We investigated their phenotypes. Intriguingly, severe loss of skeletal muscle weight, decreased myofiber number, increased fat and fibrosis volume, and apparent muscle weakness were observed in the DBA/2-*mdx* mice. These results indicate that the intrinsic genetic program affects the properties of satellite cells, and DBA/2-*mdx* will be a more useful model of DMD than C57BL/10-*mdx*. It is also speculated that the high self-renewal potential of C57BL/10 satellite cells might explain the difference in pathologies between humans and mice.

Materials and Methods

Mice

Six-week-old, specific pathogen-free, BALB/c, C3H/HeN, C57BL/6, and DBA/2 mice were purchased from Charles River Japan (Yokohama, Japan). Six-week-old, specific pathogen-free C57BL/10 mice were purchased from Shimizu Laboratory Supplies Co., Ltd (Kyoto, Japan). Specific pathogen-free *mdx* mice (of C57BL/10 background) were provided by Central Laboratories of Experimental Animals (Kanagawa, Japan) and maintained in our animal facility by brother-sister matings. *Mdx* of C57BL/10 background were backcrossed into DBA/2 genetic background. Mice backcrossed more than five generations were used in this study. Genotyping was performed according to previous reports.[16] All procedures for experimental animals were approved by the Experimental Animal Care and Use Committee at Osaka University.

Muscle Injury

Muscle injury was induced by injecting cardiotoxin (10 μmol/L in saline, Wako Pure Chemical Industries, Tokyo, Japan) into tibialis anterior (50 μl), gastrocnemius (150 μl), and quadriceps femoris (100 μl) muscles as described.[17] All injections were first done when mice were 8 to 10 weeks of age.

Histological Analysis

Tibialis anterior, gastrocnemius, and quadriceps femoris muscles were isolated and frozen in liquid nitrogen-cooled isopentane (Wako Pure Chemical Industries). Cryosections (10 μm) were stained with H&E, Oil red-O (Sigma-Aldrich, St. Louis, MO), or Sirius Red (Sigma-Aldrich).

Immunohistochemistry

For immunohistochemical examinations, transverse cryosections (6 μm) were stained with various antibodies. Monoclonal rat anti-laminin α2 (1:200; clone: 4H8-2) and mouse anti-Pax7 antibodies were purchased from Alexis Biochemical (Lausen, Switzerland) and Developmental Studies Hybridoma Bank (Iowa, IA), respectively. For Pax7 staining, a M.O.M. kit (Vector Laboratories, Burlingame, CA) was used to block endogenous mouse IgG. After the first staining at 4°C overnight, sections were reacted with secondary antibodies conjugated with Alexa 488 or Alexa 568 (Molecular Probes, Eugene, OR). Sections were shielded using Vectashield (Vector Laboratories, Inc). The signals were recorded photographically using an Axiophot microscope (Carl Zeiss, Oberkochen, Germany).

Preparation of Muscle Satellite Cells and Culture

Satellite cells were isolated from uninjured adult skeletal muscle using biotinylated-SM/C-2.6[18] and IMag methods (BD Immunocytometry Systems, Mountain View, CA) as described in a previous report.[17] Satellite cells were cultured in a growth medium of high-glucose Dulbecco's modified Eagle's medium (Sigma-Aldrich) containing 20% fetal calf serum (Trace Biosciences, N.S.W., Australia), 2.5 ng/ml basic fibroblast growth factor (Pepro-Tech, London, UK), leukemia inhibitory factor (Alexis Biochemical), and penicillin (100 U/ml)-streptomycin

(100 μg/ml) (Gibco BRL, Gaithersburg, MD) on culture dishes coated with Matrigel (BD Bioscience, San Diego, CA).

Colony Forming Assay

Clonal cultures of freshly isolated satellite cells were performed in 96-well plates coated with type I collagen (Sumilon, Tokyo, Japan) in growth medium for a week. The frequency of colony formation and number of cells in each well were counted under a phase-contrast microscope.

Cell Proliferation Assay

Isolated satellite cells were cultured in growth medium for 3 to 4 days, and expanded primary myoblasts were harvested and additional culture was performed in 96-well dishes for 1 day. Eight hours later, bromodeoxyuridine (BrdU) uptake was quantified using the Cell Proliferation ELISA, BrdU Kit (Roche Diagnostics, Basel, Switzerland) and a microplate reader (Model 680, Bio-Rad, Hercules, CA).

Measurement of Sizes of Myofibers and Oil Red-O-Positive and Fibrotic Areas

Image J software was used to measure myofiber sizes and Oil red-O- and Sirius Red-positive areas.

Evans Blue Dye Injection

Evans blue (Wako Pure Chemical Industries) was dissolved in PBS and injected intraperitoneally into mice (1 mg/100 μl/10g body weight).[19] Sixteen to 18 hours later, muscle tissues were removed, and frozen in liquid nitrogen-cooled isopentane. The muscle fibers with Evans Blue incorporated were then counted as injured muscles.

Muscle Endurance and Grip Strength Test

The muscle endurance test was referred to the studies by Handschin et al.[20] In brief, we used a MK-680S treadmill (Muromachi Kikai Co., Ltd., Tokyo, Japan). For 3 days, animals were acclimated to treadmill running for 5 minutes at a speed of 10 m/min on a 0% grade. After the acclimation, animals ran on a treadmill with a 10% uphill grade starting at a speed of 10 m/min for 5 minutes. Every subsequent 2 minutes, the speed was increased by 2 m/min until the mice were exhausted. Exhaustion was defined as the inability of the animal to remain on the treadmill despite mechanical prodding. Running time and speed were measured, and the distance was calculated. Grip strength was measured using a MK-380M grip strength meter (Muromachi Kikai Co., Ltd). The grip strength of each individual mouse was measured 10 times, the same measurements were repeated on the next day, and the highest value of each experiment was used.

Statistics

Values were expressed as means ± SD. Statistical significance was assessed by Student's *t*-test. In comparisons of more than two groups, nonrepeated measures analysis of variance (analysis of variance) followed by the Student-Newman-Keuls test were used. A probability of less than 5% ($P < 0.05$) or 1% ($P < 0.01$) was considered statistically significant.

Results

Genetic Differences in Skeletal Muscle Regeneration

To examine the long-term regeneration ability of four inbred strains of mice, repeated cycles of degeneration–regeneration were induced by injection of cardiotoxin (CTX). CTX was injected into one side of the tibialis anterior (TA), gastrocnemius (GC), and quadriceps (Qu) muscle every 2 weeks. At the last (sixth) CTX injection, another intact TA muscle received CTX once to examine the regenerative potential in one cycle of each mouse at this age. Four weeks later, the muscles were removed and analyzed. As shown in Figure 1, A and B, none of the strains displayed a striking difference in either skeletal muscle weight or histochemistry after one CTX injection (CTX-1), except for the appearance of adipocytes in BALB/c. However, the DBA/2 mice that received six CTX injections (CTX-6) exhibited remarkably impaired regeneration (Figure 1A) and loss of TA muscle weight (Figure 1B). A similar loss of muscle weight was also observed in GC and Qu of DBA/2 (CTX-6 in Figure 1C). In contrast, none of the other strains showed a significant difference in uninjured muscle weight at this age (uninjured in Figure 1C). Fat was observed in DBA/2, BALB/c, and C3H/HeN after six injections, but the sclerosis and loss of muscle weight was remarkable in DBA/2. Therefore, the following experiments were performed on C57BL/6 and DBA/2.

Regeneration Impairment in DBA/2 Is Inherited Recessively

To assess the inheritance of the lower regeneration ability of DBA/2, we injected CTX into C57BL/6, DBA/2, and their F1 mice (B6D2F1). To allow more sufficient regeneration time, the interval between CTX injections was changed to 4 weeks. As shown in Figure 2A, we found marked muscle weight loss in DBA/2 after three CTX injections (4 weeks × 3). The results of B6D2F1 mice were similar to those of C57BL/6 (Figure 2, A and B).

As shown in Figure 1A, DBA/2 mice exhibited impaired regeneration accompanied by accumulation of fat and fibrosis after three CTX injections (4 weeks × 3), but not in the 4 weeks × 1 experiment (Figure 2B). Oil red-O (Figure 2C) and Sirius Red (Figure 2D) stainings were performed to determine the amount of fat and fibrosis, respectively. As shown in Figure 2E, increments in fat and fibrotic areas were observed in DBA/2 mice receiving

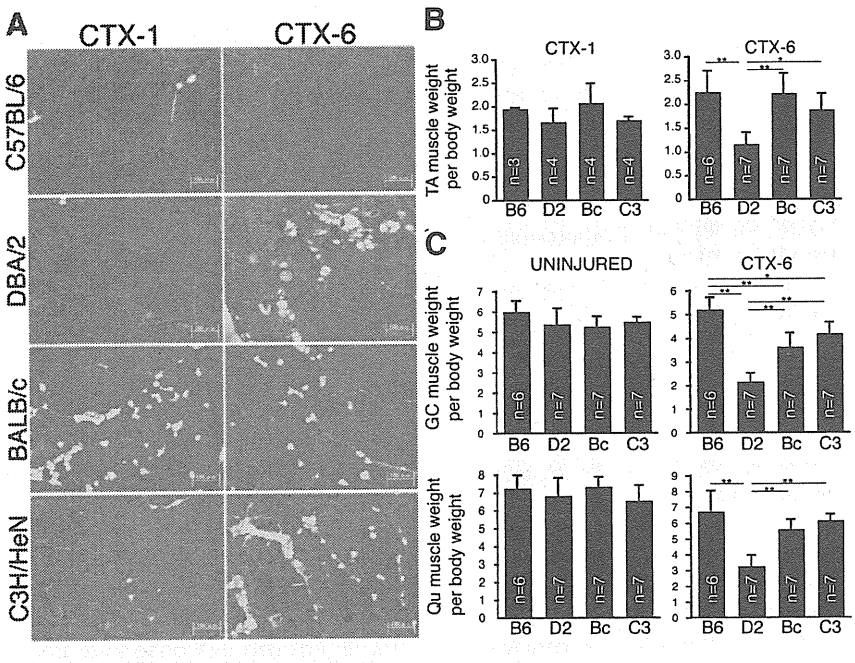

Figure 1. Impaired regeneration and loss of muscle weight in DBA/2 mice after injured six times. **A:** TA (tibialis anterior) muscles were examined histologically in four inbred strains of mice after one (CTX-1) or six (CTX-6) cardiotoxin (CTX) injections. The cross sections were stained with H&E. Scale bar =100 μm. **B:** The TA muscle weight (mg) per body weight (g) in each inbred strain after one or six CTX injections. B6, D2, Bc, and C3 indicate C57BL/6, DBA/2, BALB/c, and C3H/HeN mice, respectively. **C:** The GC (gastrocnemius) and Qu (quadriceps) muscle weights (mg) per body weight (g) in each inbred strain from uninjured or muscle injured six times. The number in the each graph indicates the number of mice used in these experiments. $^{*}P < 0.05$, $^{**}P < 0.01$ (analysis of variance, SNK-test).

three injections (4 weeks × 3). In 4 weeks × 1 DBA/2, the fat accumulation of one mouse was a slightly higher volume (2.02%), but three mice showed little fat accumulation (less than 0.6%). In contrast to DBA/2, C57BL/6, and B6D2F1 mice did not show any sign of impaired regeneration. These results indicate that the impaired regeneration ability of the DBA/2 strain after repeated injury is recessive heredity.

Loss of Muscle Mass Results from Decreased Number and Size of Myofibers

To assess the cause of muscle weight loss in DBA/2, the numbers and sizes of myofibers were quantified. In uninjured muscle, no significant difference between the numbers of myofibers was observed in C57BL/6 and DBA/2 (Figure 3A). However, as shown in Figure 3B, decreased numbers of myofibers were observed in DBA/2 after three CTX injections (4 weeks × 3), as compared with 4 weeks × 1 or uninjured muscle. C57BL/6 showed more myofibers than uninjured muscle after one or three injections (Figure 3B).

The sizes of myofibers were also measured. Four weeks after one CTX injection (4 weeks × 1), the size of myofibers in DBA/2 was similar to that in C57BL/6 (Figure 3, C and D). However, the regenerated myofibers of DBA/2 (4 weeks × 3) were slightly smaller than those of C57BL/6 (Figure 3, C and D). These data indicate that the loss of muscle weight in DBA/2 results from the decreased number and size of myofibers.

Decreased Number of Self-Renewed Satellite Cells in DBA/2

We hypothesized that a decreased number of satellite cells leads to the loss of myofibers, because myofibers are mainly made by satellite cells. To elucidate this hypothesis, we examined the number of satellite cells. As shown in Figure 3E, cells positive for Pax7, a specific marker of satellite cells,[21] lying beneath the basal lamina were counted. There was no significant difference between the uninjured TA muscles of C57BL/6 and DBA/2 mice. However, a remarkable decrease in the number of satellite cells was observed in DBA/2 after three CTX injections (Figure 3F). These results imply that the functions (including self-renewal potential) of satellite cells include responsibility for most of the regeneration of impaired muscle in DBA/2.

Colony Formation and Proliferation of Satellite Cells from DBA/2

To examine whether there is an intrinsic difference between the satellite cells of C57BL/6 and DBA/2, satellite cells were isolated and cultured *in vitro*. As shown in Figure 4A, the BrdU uptake of primary myoblasts of DBA/2 was inferior to that of C57BL/6 myoblasts. Next, we performed a colony-forming assay of single satellite cells. As shown in Figure 4C, single DBA/2 satellite cell did not produce large colonies similar to those of C57BL/6. The frequencies of colony forming cells did not differ in C57BL/6 and DBA/2 (Figure 4B). These results indicate that intrinsic factors affect the properties of satellite cells.

*Loss of Muscle Weight in DBA/2-*mdx

To assess whether the low regenerative potential of mice with the dystrophin mutation exhibit DMD-like features, we crossed C57BL/10-*mdx* (B10-*mdx*) into DBA2. It was reported that body weight of B10-*mdx* is heavier than that of the control wild-type.[22] In contrast to B10-*mdx*, DBA/

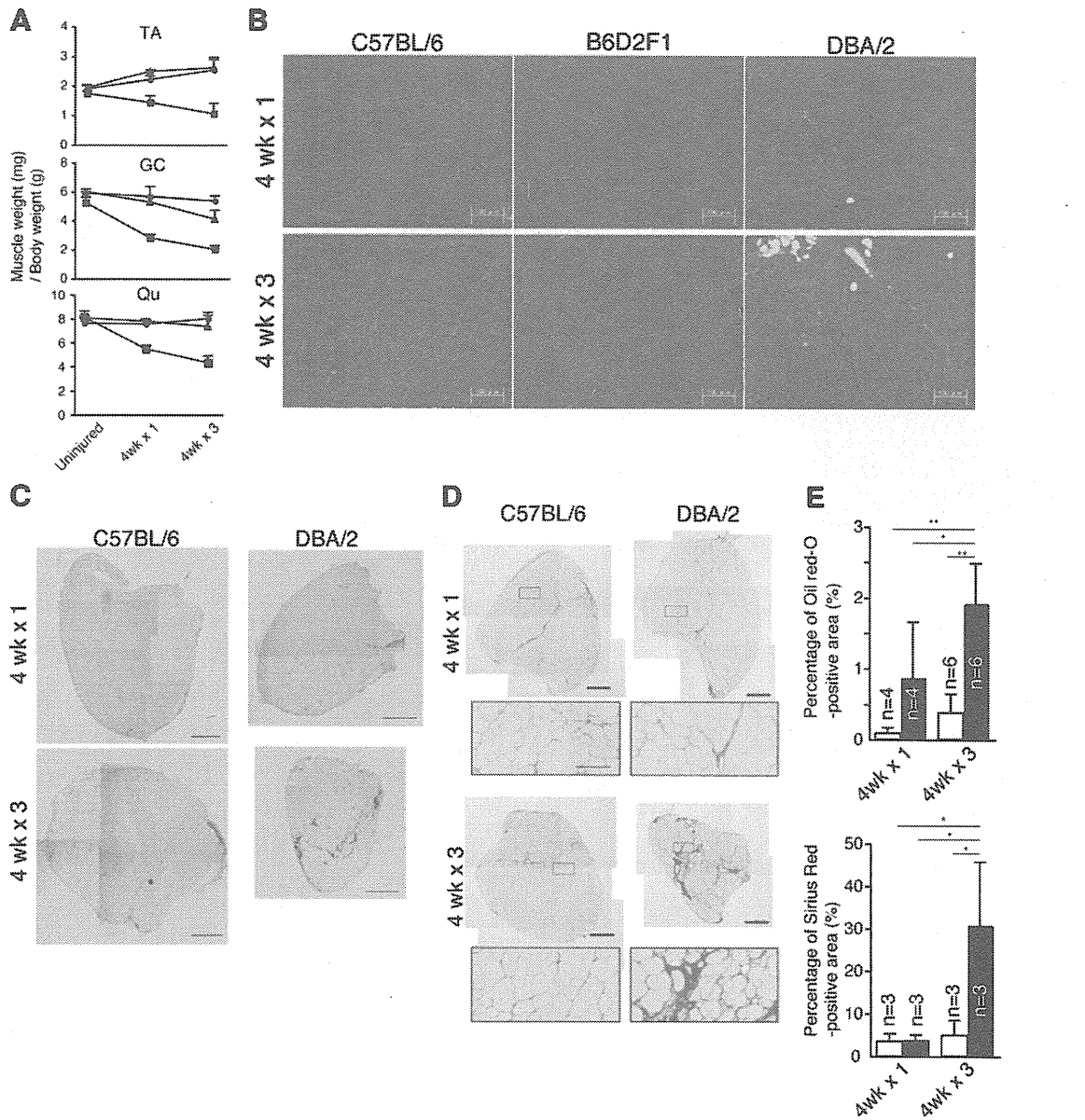

Figure 2. Impaired regeneration of DBA/2 phenotype is recessively inherited. **A:** The TA, GC, and Qu muscle weights (mg) per body weight (g) in C57BL/6 (closed circles), DBA/2 (closed squares), and B6D2F1 (closed triangles) mice after one (4 weeks × 1) or three CTX injections (4 weeks × 3). The cross sections were stained with H&E (**B**), Oil red-O (**C**), or Sirius Red (**D**). Scale bars: 100 μm (**B**); 500 μm (**C** and **D**). **E:** The *y* axis shows the mean percentage of Oil red-O or Sirius Red-positive areas per section. White and black columns indicate the results of C57BL/6 and DBA/2, respectively. The number in the each graph indicates the number of mice used in this analysis. $^{*}P < 0.05$, $^{**}P < 0.01$ (analysis of variance, SNK-test).

2-*mdx* (D2-*mdx*) mice showed the decreased body weight regardless of gender (Figure 5A). A more remarkable phenotype of D2-*mdx* was the loss of skeletal muscle mass (Figure 5B). As previously reported, the muscle weight of B10-*mdx* was heavier than that of controls,[8] but the TA, GC, and Qu muscle weights of D2-*mdx* males were 71%, 59%, and 54% of those of controls, respectively (Figure 5C). Female muscles were 85% (TA), 61% (GC), and 52% (Qu) of each control muscle, respectively. The loss of muscle weight did not simply reflect the decreased body weight because there is also a significant difference in muscle weight (mg) per body weight (g) between D2-*mdx* and control littermates (Figure 5C). Control littermates of D2-*mdx* and normal DBA/2 exhibited similar results in muscle weight per body weight ratios (data not shown).

Histology of DBA/2-mdx

In contrast to the histology of DMD, it is widely accepted that fibrosis and fat replacement are minimal in B10-*mdx*.[7] In addition, there was no apparent fiber loss. To examine the accumulation of fibrosis and fat tissue in D2-*mdx*, cross sections were stained with Sirius Red or Oil red-O. As shown in Figure 6, A and B, there was no sign of fibrosis or adipogenesis in B10-*mdx*. However, D2-*mdx* mice exhibited increased fibrosis and fat accu-

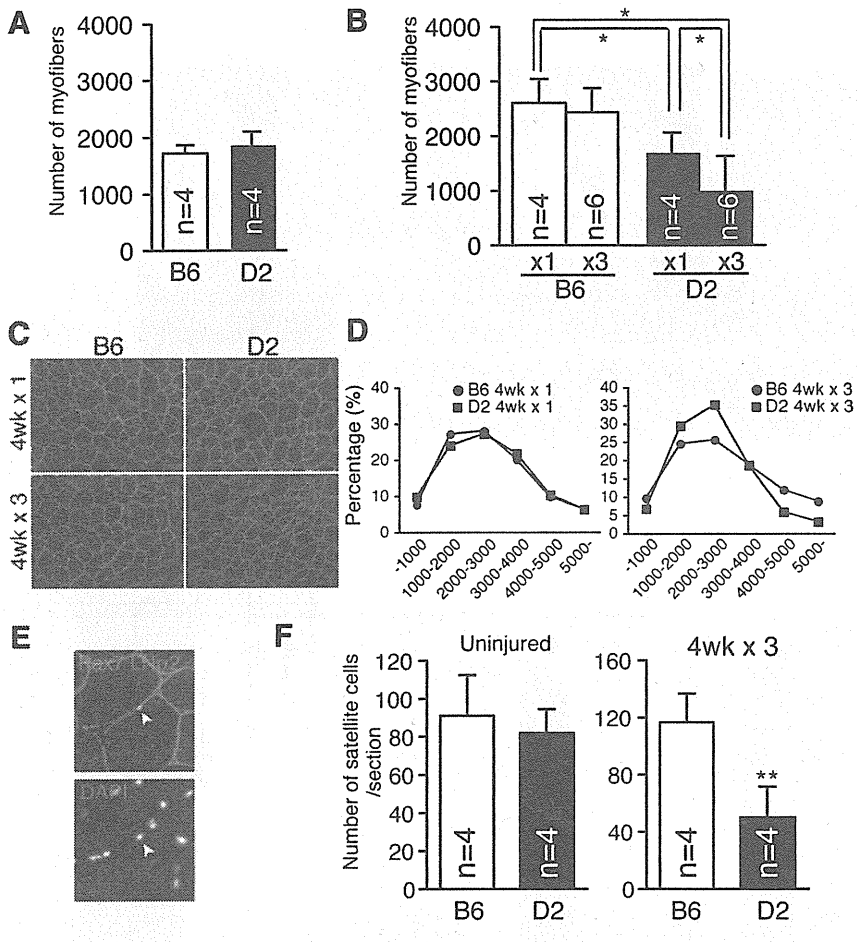

Figure 3. Decreased numbers of myofibers and satellite cells in DBA/2 mice after three repeated injuries. **A:** The number of myofibers in uninjured TA muscle at 10 weeks old. The *y* axis shows the mean number of myofibers per section. B6 and D2 indicate C57BL/6 and DBA/2, respectively. **B:** The mean numbers of myofiber in TA muscles after one or three injuries. $^{*}P < 0.05$ (analysis of variance, SNK-test). The sizes of myofibers in TA muscle after one or three CTX injections. **C:** Cross sections were stained with anti-laminin α2 antibody (green). **D:** The size of each myofiber in TA muscle was measured after one or three injections. Closed circles or squares show the results of C57BL/6 or DBA/2, respectively. **E: Arrowhead** indicates Pax7 expressing cells lying beneath the basal lamina. **F:** The number of satellite cells in noninjured TA muscle (uninjured) or TA muscle injured three times (4 weeks × 3). The *y* axis shows the mean number of satellite cells per section. The number in each graph indicates the number of mice used in these analyses. $^{**}P < 0.01$ (Student's *t*-test).

mulation in comparison with B10-*mdx*. In contrast to B10-*mdx*, a decreased number of total myofibers was also observed in D2-*mdx* (Figure 6C).

To enumerate the number of necrotic fibers, the mice were injected with Evans blue dye to visualize necrotic fibers. As shown in Figure 6C, fewer total necrotic fibers were observed in D2-*mdx*. This result suggests that the D2-*mdx* phenotype does not result from acceleration of degeneration.

Decreased Skeletal Muscle Function in DBA/2-mdx

Skeletal muscle endurance was assessed by treadmill running to exhaustion as an indicator of maximal muscle capacity. After acclimatization, mice were run on a 10% slope at increasing speed until the animals were unable to remain on the treadmill despite prodding. We then recorded the end time and speed to calculate the distance run. As shown in Figure 7A, male and female D2-*mdx* ran 45% and 56% shorter distances than control littermates. The maximum speed of D2-*mdx* was also lower than that of their littermate. The distance run showed the most significantly difference because of the protocol of increasing speed (Figure 7A). The average distance run by male controls was 544 meters, but that of D2-*mdx* males was 205 meters (38% of the control). A similar result was shown by female D2-*mdx* (25% of the control). B10-*mdx* also showed lower values compared with normal C57BL/10 mice (data not shown), but the decreased ratio of each parameter in D2-*mdx* was more remarkable than that in B10-*mdx* (Figure 7B).

A grip strength test was also performed as an indicator of motor function and whether D2-*mdx* exhibited muscle weakness compared with controls. As shown in Figure 7C, D2-*mdx* earned a lower score than control mice regardless of gender. However, there was no significant difference between B10-*mdx* and control mice.

Discussion

Repeated Injury Models

Muscle satellite cells play central roles in skeletal muscle regeneration.[23] Satellite cells produce a vast number of progenitor cells (myoblasts) that finally become myofibers. During this process, at least some of the satellite cells have self-renewal potential,[14,24] but are quiescent and will respond efficiently to the next damages. In fact, Luz et al[15] indicated that C57BL/10 could regenerate after 50 bupivacaine injections without the loss of myofibers or gain of fibrotic areas in the TA muscle. Importantly, C57BL/10-*mdx* mice exhibited decreased numbers of myofibers after 50 bupivacaine injections[15]

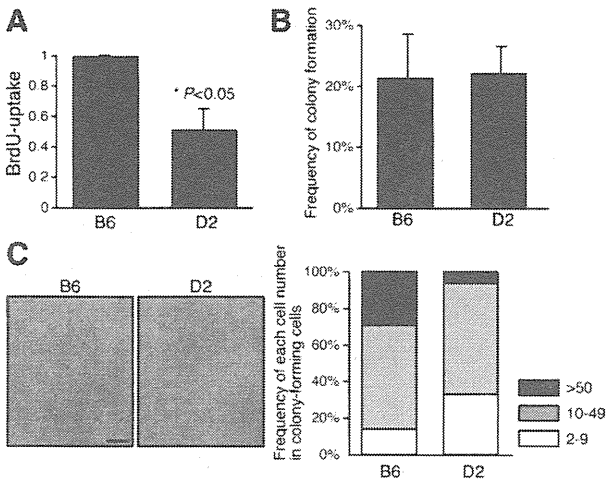

Figure 4. Satellite cells of DBA/2 strain show inferior BrdU uptake and colony-forming potential. **A:** BrdU uptake of primary myoblasts derived from C57BL/6 or DBA/2 satellite cells. The *y* axis shows the mean with SD of three independent experiments. $^{*}P < 0.05$ (Student's *t*-test). Frequency of colony formation by a single satellite cell derived from C57BL/6 or DBA/2 (**B**) and the size of single cell-derived colonies (**C**). The picture shows representative colonies of each strain. Colonies were categorized into three groups: >50 cells/well, 10 to 49 cells/well, and 2 to 9 cells/well. The *y* axis indicates the frequency (**B**) or percentage of each category (**C**) from three independent experiments. Scale bar = 100 μm.

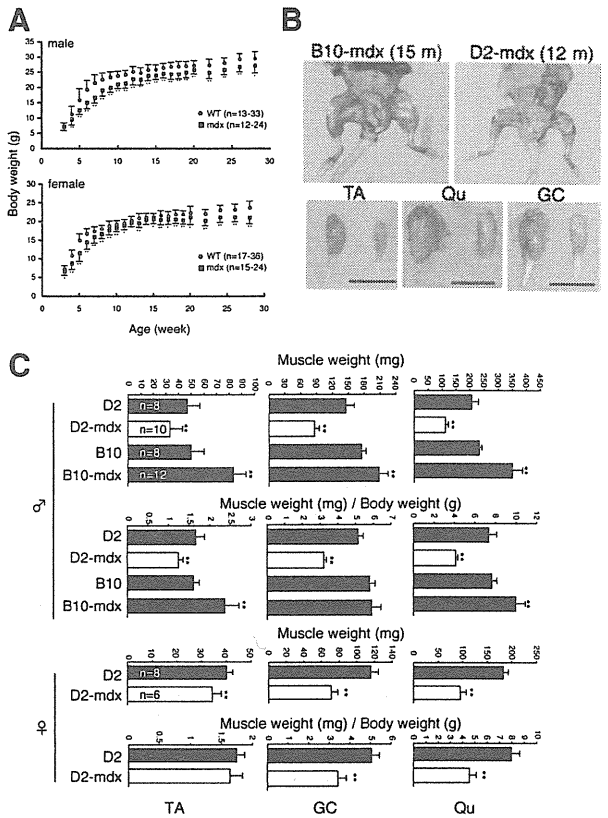

Figure 5. DBA/2-*mdx* mice show decreased body weight and remarkable muscle weight loss. **A:** Body weight of D2-*mdx* (closed squares) and their wild or heterozygous littermates (open circles) related to age. $^{*}P < 0.05$, $^{**}P < 0.01$ (Student's *t*-test) **B:** Photographs of hind limb muscles of male B10-*mdx* (15 months) and D2-*mdx* (12 months). Scale bar = 1 cm. **C:** TA, GC, and Qu muscle weights (mg) or per body weight (g) of 6-month-old mice. *x* axis shows the mean with SD. The numbers of muscles used in each study are shown in each graph. $^{*}P < 0.05$, $^{**}P < 0.01$.

because C57BL10-*mdx* mice already have dystrophic degeneration–regeneration cycles. Sadeh et al[25] also showed active regeneration cycles in rats that received weekly injections of bupivacaine for 6 months. They reported that there was lack of evidence for reduction or exhaustion of muscle fiber capacity to regenerate despite ongoing degeneration–regeneration over a period approximating one fourth of the rat life expectancy. These results indicate that the satellite cell pool was efficiently maintained for multiple degeneration–regeneration cycles in these animals, and that dystrophic mice exhibit less regeneration ability. However, DBA/2 showed significantly decreased numbers of myofibers and self-renewed satellite cells after only three injections of CTX.

The number of DBA/2 satellite cells in uninjured TA muscle is similar to that of C57BL/6. Although, the myofibers in DBA/2 were smaller than those in C57BL/6 2 weeks after one CTX injection (data not shown), the myofiber size and histological characteristics showed few significant differences between and DBA/2 and C57BL/6 4 weeks after a single CTX injection. These results suggest that the self-renewal ability of DBA/2 satellite cells is incomplete and that the exhaustion of muscle satellite cells leads to a decreased number of myofiber and loss of skeletal muscle weight. Nonmyogenic cells, for example, macrophages, also play important roles in skeletal muscle regeneration. However, dysfunction of macrophages leads to impaired regeneration after one CTX injection.[26,27] Furthermore, the remarkable regeneration deficit was not observed in DBA/2 4 weeks after one CTX injection in TA muscle. These results suggest that repeated injury is a suitable model to assess the long-term regeneration potential of skeletal muscle, and that the self-renewal ability of satellite cells is responsible at least in part for the result of repeatedly injured muscle in DBA/2.

Strain Differences of Muscle Regeneration Ability

C57BL/6, a strain akin to C57BL/10, is the most widely used strain for skeletal muscle regeneration studies. As shown in Figure 1, C57BL/6 has the best ability to regenerate skeletal muscle among the four inbred strains examined. An early study by Grounds and McGeachie[28] indicated a strain difference in skeletal muscle regeneration between BALB/c and Swiss SJL/J. They showed that superior and faster regeneration was observed in the Swiss SJL/J strain. The most outstanding phenotype of DBA/2 is the remarkable decrease of muscle weight compared with the three other inbred strains, including BALB/c. Intriguingly, DBA/2 mice have a shorter life span than C57BL/6.[29] In addition, it is reported that muscle weight loss is increased during aging (sarcopenia) in DBA/2 mice compared with C57BL/6.[30] The reason why the DBA/2 strain exhibits the loss of muscle weight is unknown, but our results imply a relationship between

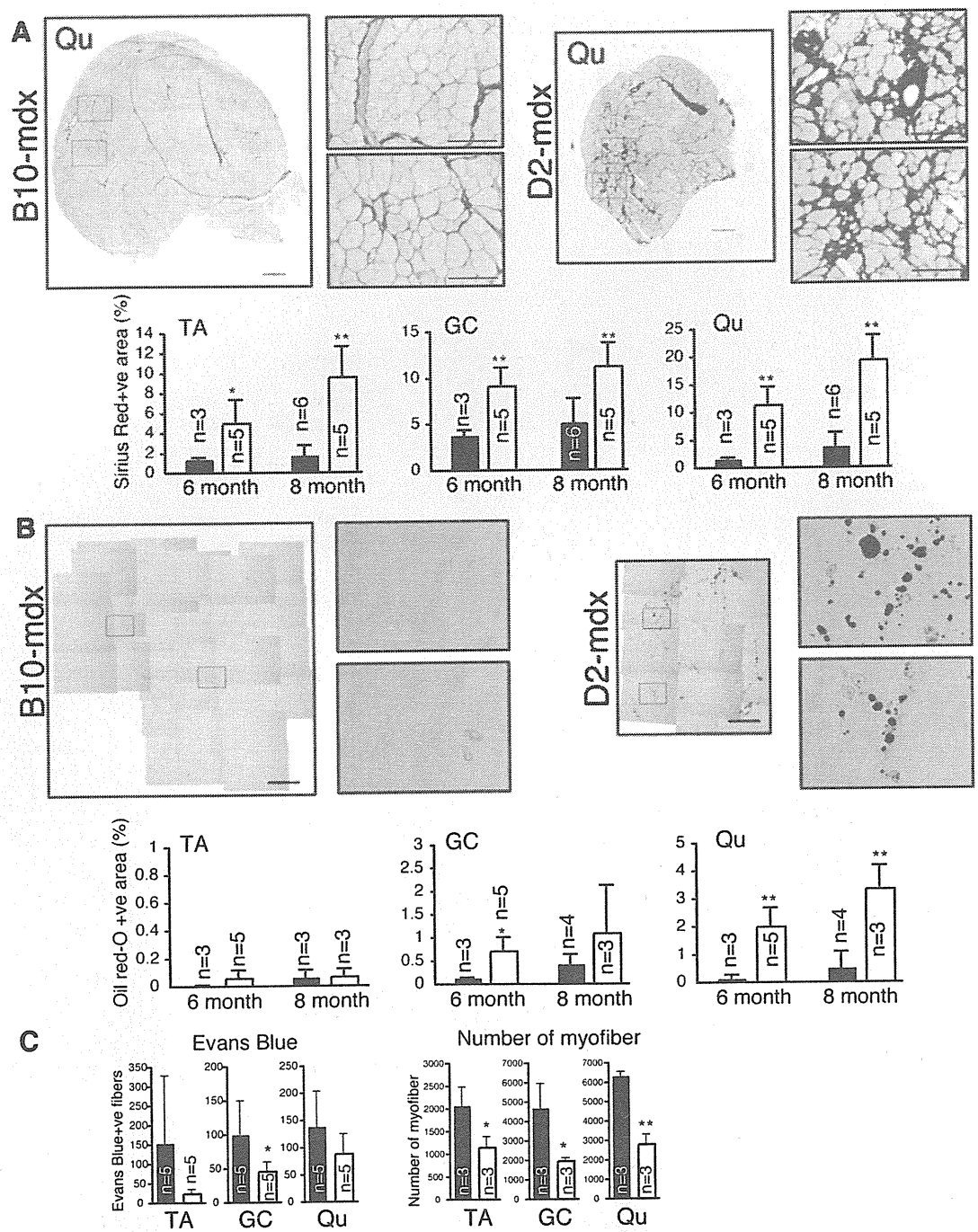

Figure 6. Histological analyses of DBA/2-*mdx* mice. Sirius red staining (**A**) and Oil red-O staining (**B**) of Qu muscle of 8-month-old B10-*mdx* and D2-*mdx* mice. The *y* axis indicates the mean percentage of Sirius Red- (**A**) or Oil red-O (**B**) -positive areas per section. The *x* axis indicates the age of mice. Black and white columns show the results for B10-*mdx* and D2-*mdx*, respectively. The numbers of mice used in each study are shown in each graph. **C:** The *y* axis indicates the mean number of Evans blue-positive or total myofibers of B10-*mdx* and D2-*mdx* at 8 months of age. $^{*}P < 0.05$, $^{**}P < 0.01$.

the impaired function of satellite cells and sarcopenia in DBA/2.

Heydemann et al[31] reported that γ-sarcoglycan-null mice with DBA/2 background showed decreased skeletal muscle weight, increased Evans Blue uptake, and a higher hydroxyproline concentration than C57BL/6, CD1, and 129 background null mice. Although they ruled out the voluntary activities of DBA/2, they did not discuss the cause of these results. Our results suggest that the low regeneration potential of DBA/2 leads to a severe skeletal muscle phenotype in various dystrophic mouse models.

The DBA/2J strain has been used in sarcopenia and γ-sarcoglycan-null mouse studies.[30,31] To exclude the possibility that DBA/2 substrain differences exist, we compared the BrdU uptake of primary myoblasts in DBA/2N (used in this study) and DBA/2J. Because we observed similar low BrdU uptakes by primary myoblasts in both DBA/2N and DBA/2J (data not shown), these

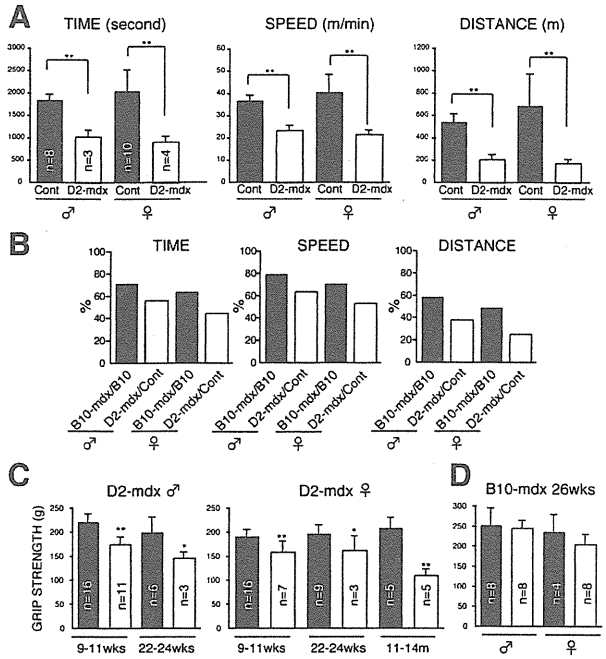

Figure 7. Comparison of muscle strength in DBA/2-*mdx* and B10-*mdx*. **A:** Treadmill running test of mice at 24 weeks old. Final time, speed, and distance were recorded and calculated for the individual performance score. The averages are shown with SD. Control indicates heterozygous or wild-type littermates of D2-*mdx*. The numbers of mice used in each study are shown in each graph. $^{*}P < 0.05$, $^{**}P < 0.01$. **B:** Comparison of C57BL/10-*mdx* and DBA/2-*mdx* in treadmill running test. The *y* axis indicates the percentage of *mdx* per control value. The numbers of male C57BL/10, male C57BL/10-*mdx*, female C57BL/10, and female C57BL/10-*mdx* are 4, 4, 4, and 8, respectively. Grip strength test of D2-*mdx* (**C**) or B10-*mdx* (**D**). Black and white columns indicate the results for *mdx* or control mice, respectively. The *y* axis indicates the average score of each mouse with SD. The *x* axis shows the ages of mice. The number in the each graph indicates the number of mice taking this test. $^{*}P < 0.05$, $^{**}P < 0.01$.

results suggest that lower muscle regeneration is common to the DBA/2 strain.

Stem (Satellite) Cell Function and Mouse Strains

As mentioned above, some previous reports indicated different responses in skeletal muscle regeneration among inbred strains of mice. However, to our knowledge, this is the first evidence that there is an intrinsic difference in satellite cells among inbred mice. The exact relationship between *in vitro* and *in vivo* results of satellite cells is not clear. However, low or slow proliferation of satellite cells might explain the decreased muscle weight and slow regeneration after a single injury in DBA/2 in comparison with C57BL/6 and B6D2F1, which showed increased muscle weight in their TA muscle (Figure 2A). It is unlikely that telomere erosion contributes to the *in vitro* and *in vivo* results of DBA/2 satellite cells because DBA/2 mice have longer telomeres than C57BL/6 mice.[32]

Recently Kuang et al[33] reported that satellite cells are a heterogeneous population of stem cells (satellite stem cells) and committed progenitor cells, and that they can be distinguished from others by Myf5 expression. They showed that Myf5-negative (satellite stem) cells self-renewed three times more frequently than Myf-5-positive (progenitor) cells *in vivo*. Schultz and Lipton[34] first described the heterogeneity of satellite cells by the different colony sizes of each satellite cell and found decreased colony sizes in aging muscle in the rat. Although it was not determined whether satellite stem cells form a large-colonies or not *in vitro*, our results showed that mice having low self-renewing satellite cells (DBA/2) exhibit smaller colony formations than mice having high self-renewing satellite cells (C57BL/6). These results suggest that satellite stem cells may form larger colonies *in vitro*.

In contrast to satellite cells, a highly strain-dependent function of hematopoietic stem cells was reported.[35] Chen et al[36] reported that DBA/2 showed a decline in primitive hematopoietic stem cell function with age, but that it increased with age in C57BL/6 in a *vivo* transplantation study. Recombinant inbred mice, named BXD strains, are available. Using BXD, Liang et al[37] identified latexin as affecting the size of the hematopoietic stem cell population in mice. A similar approach might lead to the discovery of key genes that affect the properties of satellite cells.

DBA/2-mdx *as Model for DMD*

Mdx was discovered a quarter of a century ago.[5] In 1989, the *mdx* mutation, a C to T transition within exon 23, was identified in the dystrophin gene on the X chromosome.[38] Nearly all *mdx* colonies are maintained as homozygous inbred lines; in addition, the difficulty of point mutation typing might impede the effect of genetic background on *mdx* phenotype. However, Amalfitano and Chamberlain[16] reported a rapid and simple typing strategy, and we established DBA/2-*mdx* following their protocol. C57BL/10-*mdx* mice have played central roles in a vast array of pathological, clinical, and physiological studies as a model for DMD. However, they do not reflect human pathology in some aspects, including little fat and fibrosis accumulation, no loss of myofiber numbers, and muscle weight. Recently, Gargioli et al[39] showed that the advanced stage of dystrophy including sclerosis precluded treatment by stem cell therapy. Therefore, assessment of therapeutic effect in more severe disease conditions is needed.

In marked contrast to the severe phenotype observed in DMD, early studies using C57BL/10-*mdx* concluded that they do not show obvious functional disability.[5,7] However, some later reports indicated functional differences between C57BL/10-*mdx* and control mice.[40–43] As shown in Figure 7, C57BL/6-*mdx* also showed muscle weakness in the treadmill test. However, the muscle weakness of DBA/2-*mdx* is more remarkable than that of C57BL/10-*mdx*. Therefore, DBA/2-*mdx* is a more appropriate model to assess skeletal muscle function after therapeutic treatment.

Chamberlain et al[44] reported that the average life spans of female and male C57BL/10-*mdx* mice were 22.5 and 21.5 months, respectively. Pastoret et al[8] also reported that C57BL/10-*mdx* mice have short life spans and that C57BL/10-*mdx* older than 78 weeks exhibit progressive weakness. We have not determined the life span of DBA/2-*mdx*, but it will be clarified in the future. Intrigu-

ingly, Chamberlain et al[44] observed the appearance of rhabdomyosarcoma-like tumors in C57BL/10-*mdx*. They speculate that the lifelong continuous myofiber degeneration and regeneration that characterize this animal model are associated with continuous and massive activation and proliferation of satellite cells, which greatly increase the chance of developing random and spontaneous mutations. To date, we have observed tumors in C57BL/10-*mdx* but not in DBA/2-*mdx*. This observation supports their speculations.

The reasons why *mdx* mice do not show the human-like pathology have been investigated. One reason for the difference between DMD and *mdx* is explained by the presence of utrophin, a homolog of dystrophin. Utrophin is located in the neuromuscular junction in normal muscle. In dystrophic muscle, utrophin is up-regulated in the sarcolemma and compensates for dystrophin function. As shown in Figure 6, the results of Evans blue uptake in DBA/2-*mdx* indicated that the degeneration of myofiber was not accelerated, but that the regeneration potential was inferior. These results clearly indicate that not only utrophin expression but also regeneration potential, perhaps a satellite cell function, directly leads to the pathological condition. The identification of genes that determine the DBA/2 phenotype will provide new therapeutic strategies for the treatment of muscular dystrophy.

Acknowledgment

We thank Katherine Ono for reading this manuscript.

References

1. Koenig M, Monaco AP, Kunkel LM: The complete sequence of dystrophin predicts a rod-shaped cytoskeletal protein. Cell 1988, 53:219–228
2. Suzuki A, Yoshida M, Hayashi K, Mizuno Y, Hagiwara Y, Ozawa E: Molecular organization at the glycoprotein-complex-binding site of dystrophin. Three dystrophin-associated proteins bind directly to the carboxy-terminal portion of dystrophin. Eur J Biochem 1994, 220:283–292
3. Ervasti JM, Campbell KP: A role for the dystrophin-glycoprotein complex as a transmembrane linker between laminin and actin. J Cell Biol 1993, 122:809–823
4. Carpenter S, Karpati G: Disease of skeletal muscle. Edited by S Carpenter, G Karpati. New York, Oxford University Press, Inc., 2001, pp. 373–524
5. Bulfield G, Siller WG, Wight PA, Moore KJ: X chromosome-linked muscular dystrophy (mdx) in the mouse. Proc Natl Acad Sci USA 1984, 81:1189–1192
6. Stedman HH, Sweeney HL, Shrager JB, Maguire HC, Panettieri RA, Petrof B, Narusawa M, Leferovich JM, Sladky JT, Kelly AM: The mdx mouse diaphragm reproduces the degenerative changes of Duchenne muscular dystrophy. Nature 1991, 352:536–539
7. Tanabe Y, Esaki K, Nomura T: Skeletal muscle pathology in X chromosome-linked muscular dystrophy (mdx) mouse. Acta Neuropathol 1986, 69:91–95
8. Pastoret C, Sebille A: mdx mice show progressive weakness and muscle deterioration with age. J Neurol Sci 1995, 129:97–105
9. Deconinck AE, Rafael JA, Skinner JA, Brown SC, Potter AC, Metzinger L, Watt DJ, Dickson JG, Tinsley JM, Davies KE: Utrophin-dystrophin-deficient mice as a model for Duchenne muscular dystrophy. Cell 1997, 90:717–727
10. Grady RM, Teng H, Nichol MC, Cunningham JC, Wilkinson RS, Sanes JR: Skeletal and cardiac myopathies in mice lacking utrophin and dystrophin: a model for Duchenne muscular dystrophy. Cell 1997, 90:729–738
11. Bischoff R: Analysis of muscle regeneration using single myofibers in culture. Med Sci Sports Exerc 1989, 21:S164–172
12. Mauro A: Satellite cell of skeletal muscle fibers. J Biophys Biochem Cytol 1961, 9:493–495
13. Schultz E, Gibson MC, Champion T: Satellite cells are mitotically quiescent in mature mouse muscle: an EM and radioautographic study. J Exp Zool 1978, 206:451–456
14. Collins CA, Olsen I, Zammit PS, Heslop L, Petrie A, Partridge TA, Morgan JE: Stem cell function, self-renewal, and behavioral heterogeneity of cells from the adult muscle satellite cell niche. Cell 2005, 122:289–301
15. Luz MA, Marques MJ, Santo Neto H: Impaired regeneration of dystrophin-deficient muscle fibers is caused by exhaustion of myogenic cells. Braz J Med Biol Res 2002, 35:691–695
16. Amalfitano A, Chamberlain JS: The mdx-amplification-resistant mutation system assay, a simple and rapid polymerase chain reaction-based detection of the mdx allele. Muscle Nerve 1996, 19:1549–1553
17. Fukada S, Yamamoto Y, Segawa M, Sakamoto K, Nakajima M, Sato M, Morikawa D, Uezumi A, Miyagoe-Suzuki Y, Takeda S, Tsujikawa K, Yamamoto H: CD90-positive cells, an additional cell population, produce laminin alpha2 upon transplantation to dy(3k)/dy(3k) mice. Exp Cell Res 2008, 314:193–203
18. Fukada S, Higuchi S, Segawa M, Koda K, Yamamoto Y, Tsujikawa K, Kohama Y, Uezumi A, Imamura M, Miyagoe-Suzuki Y, Takeda S, Yamamoto H: Purification and cell-surface marker characterization of quiescent satellite cells from murine skeletal muscle by a novel monoclonal antibody. Exp Cell Res 2004, 296:245–255
19. Matsuda R, Nishikawa A, Tanaka H: Visualization of dystrophic muscle fibers in mdx mouse by vital staining with Evans blue: evidence of apoptosis in dystrophin-deficient muscle. J Biochem 1995, 118:959–964
20. Handschin C, Chin S, Li P, Liu F, Maratos-Flier E, Lebrasseur NK, Yan Z, Spiegelman BM: Skeletal muscle fiber-type switching, exercise intolerance, and myopathy in PGC-1alpha muscle-specific knock-out animals. J Biol Chem 2007, 282:30014–30021
21. Seale P, Sabourin LA, Girgis-Gabardo A, Mansouri A, Gruss P, Rudnicki MA: Pax7 is required for the specification of myogenic satellite cells. Cell 2000, 102:777–786
22. Connolly AM, Keeling RM, Mehta S, Pestronk A, Sanes JR: Three mouse models of muscular dystrophy: the natural history of strength and fatigue in dystrophin-, dystrophin/utrophin-, and laminin alpha2-deficient mice. Neuromuscul Disord 2001, 11:703–712
23. Charge SB, Rudnicki MA: Cellular and molecular regulation of muscle regeneration. Physiol Rev 2004, 84:209–238
24. Sacco A, Doyonnas R, Kraft P, Vitorovic S, Blau HM: Self-renewal and expansion of single transplanted muscle stem cells. Nature 2008, 456:502–506
25. Sadeh M, Czyewski K, Stern LZ: Chronic myopathy induced by repeated bupivacaine injections. J Neurol Sci 1985, 67:229–238
26. Arnold L, Henry A, Poron F, Baba-Amı Y, van Rooijen N, Plonquet A, Gherardi RK, Chazaud B: Inflammatory monocytes recruited after skeletal muscle injury switch into anti-inflammatory macrophages to support myogenesis. J Exp Med 2007, 204:1057–1069
27. Segawa M, Fukada S, Yamamoto Y, Yahagi H, Kanematsu M, Sato M, Ito T, Uezumi A, Hayashi S, Miyagoe-Suzuki Y, Takeda S, Tsujikawa K, Yamamoto H: Suppression of macrophage functions impairs skeletal muscle regeneration with severe fibrosis. Exp Cell Res 2008, 314:3232–3244
28. Grounds MD, McGeachie JK: A comparison of muscle precursor replication in crush-injured skeletal muscle of Swiss and BALBc mice. Cell Tissue Res 1989, 255:385–391
29. Gelman R, Watson A, Bronson R, Yunis E: Murine chromosomal regions correlated with longevity. Genetics 1988, 118:693–704
30. Lionikas A, Blizard DA, Vandenbergh DJ, Stout JT, Vogler GP, McClearn GE, Larsson L: Genetic determinants of weight of fast- and slow-twitch skeletal muscles in old mice. Mamm Genome 2006, 17:615–628
31. Heydemann A, Huber JM, Demonbreun A, Hadhazy M, McNally EM: Genetic background influences muscular dystrophy. Neuromuscul Disord 2005, 15:601–609
32. Manning EL, Crossland J, Dewey MJ, Van Zant G: Influences of

inbreeding and genetics on telomere length in mice. Mamm Genome 2002, 13:234–238
33. Kuang S, Kuroda K, Le Grand F, Rudnicki MA: Asymmetric self-renewal and commitment of satellite stem cells in muscle. Cell 2007, 129:999–1010
34. Schultz E, Lipton BH: Skeletal muscle satellite cells: changes in proliferation potential as a function of age. Mech Ageing Dev 1982, 20:377–383
35. Dykstra B, de Haan G: Hematopoietic stem cell aging and self-renewal. Cell Tissue Res 2008, 331:91–101
36. Chen J, Astle CM, Harrison DE: Genetic regulation of primitive hematopoietic stem cell senescence. Exp Hematol 2000, 28:442–450
37. Liang Y, Jansen M, Aronow B, Geiger H, Van Zant G: The quantitative trait gene latexin influences the size of the hematopoietic stem cell population in mice. Nat Genet 2007, 39:178–188
38. Sicinski P, Geng Y, Ryder-Cook AS, Barnard EA, Darlison MG, Barnard PJ: The molecular basis of muscular dystrophy in the mdx mouse: a point mutation. Science 1989, 244:1578–1580
39. Gargioli C, Coletta M, De Grandis F, Cannata SM, Cossu G: PlGF-MMP-9-expressing cells restore microcirculation and efficacy of cell therapy in aged dystrophic muscle. Nat Med 2008, 14:973–978
40. Muntoni F, Mateddu A, Marchei F, Clerk A, Serra G: Muscular weakness in the mdx mouse. J Neurol Sci 1993, 120:71–77
41. Hara H, Nolan PM, Scott MO, Bucan M, Wakayama Y, Fischbeck KH: Running endurance abnormality in mdx mice. Muscle Nerve 2002, 25:207–211
42. Carter GT, Wineinger MA, Walsh SA, Horasek SJ, Abresch RT, Fowler WM, Jr.: Effect of voluntary wheel-running exercise on muscles of the mdx mouse, Neuromuscul Disord 1995, 5:323–332
43. Lynch GS, Hinkle RT, Chamberlain JS, Brooks SV, Faulkner JA: Force and power output of fast and slow skeletal muscles from mdx mice 6–28 months old. J Physiol 2001, 535:591–600
44. Chamberlain JS, Metzger J, Reyes M, Townsend D, Faulkner JA: Dystrophin-deficient mdx mice display a reduced life span and are susceptible to spontaneous rhabdomyosarcoma. FASEB J 2007, 21:2195–2204

JPSA
Japan Poultry Science Association

http://www.jstage.jst.go.jp/browse/jpsa
doi:10.2141/jpsa.46.95

Expression Pattern of *WWP1* in Muscular Dystrophic and Normal Chickens

Hirokazu Matsumoto[1], Hideaki Maruse[1], Shinji Sasazaki[1], Akira Fujiwara[2], Shin'ichi Takeda[3], Nobutsune Ichihara[4,5], Tateki Kikuchi[3], Fumio Mukai[1] and Hideyuki Mannen[1]

[1] Laboratory of Animal Breeding and Genetics, Graduate School of Agricultural Science, Kobe University, Kobe 657-8501, Japan
[2] Laboratory Animal Research Station, Nippon Institute for Biological Science, Kobuchisawa 408-0041, Japan
[3] Department of Molecular Therapy and of [4] Animal Models for Human Disease, National Institute of Neuroscience, NCNP, Kodaira, Tokyo 182-8502, Japan
[5] Department of Anatomy I, School of veterinary medicine, Azabu University, Fuchinobe, Sagamihara, Kanagawa 229-8501, Japan

The WW domain containing E3 ubiquitin protein ligase 1 (WWP1) is classified into one of ubiquitin ligases which play an important role in ubiquitin-proteasome pathway. Previously, we identified the *WWP1* gene as a candidate gene of chicken muscular dystrophy by linkage analysis and sequence comparison. However, the mechanism causing pathological changes and underlaying gene function remains elucidated. In the present study, we analyzed the *WWP1* gene expression in various muscles and tissues of normal chickens, and compared with those from muscular dystrophic chickens. Two mRNA isoforms were detected in all tissues examined and revealed almost equal expression level. The *WWP1* expression of dystrophic chickens was decreased in almost all skeletal muscles including unaffected muscles. These data indicate that there might not be a causal relationship between the alteration of *WWP1* expression level and the severity of muscular dystrophy.

Key words: chicken, expression analysis, fast twitch muscle fiber, muscular dystrophy, WWP1

J. Poult. Sci., 46: 95-99, 2009

Introduction

The WW domain containing E3 ubiquitin protein ligase 1 (*WWP1*) is classified into an ubiquitin ligase (E3) which plays an important role in ubiquitin-proteasome pathway (UPP) to degrade unneeded or damaged proteins (Scheffner and Staub, 2007). E3 recognizes and catalyzes ubiquitin (Ub) conjugation to specific protein substrates (Liu, 2004). Comparative genome analysis reveals few genes encoding E1, tens of E2 encoding genes and hundreds of E3 encoding genes (Semple *et al.*, 2003).

The *WWP1* gene is classified into HECT (homologous to the E6-AP carboxyl terminus)-type E3 which possesses one C2 domain, multiple WW domains and one HECT domain (Pirozzi *et al.*, 1997; Flasza *et al.*, 2002). The C 2 domain binds to the cellular membranes in a Ca^{2+}-dependent manner (Plant *et al.*, 1997) and mediates interactions with other proteins (Plant *et al.*, 2000; von Poser *et al.*, 2000; Augustine, 2001). The WW domain has two conserved tryptophan residues and binds proline-rich region (Sudol *et al.*, 1985). HECT domain, similar to E2s structurally, has a cysteine residue as an active center that transfers the activated Ub from E2 onto first itself, and then onto its substrates (Jackson *et al.*, 2000).

The muscular dystrophies are the group of inherited diseases with progressive weakness and degeneration of skeletal muscle (Partridge, 1991). It is well known that abnormalities of muscle proteins linking sarcolemma and basal lamina lead to cause muscular dystrophies (Lisi and Cohn, 2007), but there are a number of muscular dystrophies and related diseases of which causes are still unknown. We identified *WWP1* gene as a candidate responsible for the chicken muscular dystrophy by the linkage analysis (Matsumoto *et al.*, 2007) and the sequence comparison between normal and dystrophic chickens (Matsumoto *et al.*, 2008). The R441Q missense mutation was found in *WWP1* gene to cause the phenotype of muscular dystrophy.

The WWP1s of human (Flasza *et al.*, 2002; Komuro *et al.*, 2004), mouse (Dallas *et al.*, 2006) and *C. elegans* (Huang *et al.*, 2000) were intensively studied and known

Received: October 10, 2008, Accepted: December 24, 2008
Correspondence: Dr. H. Mannen, Graduate School of Agricultural Science, Kobe University, Kobe 657-8501, Japan.
(E-mail: mannen@kobe-u.ac.jp)

that the *WWP1* gene is expressed ubiquitously, but strongly in liver, bone marrow, testis and skeletal muscles (Flasza *et al.*, 2002; Komuro *et al.*, 2004). In chicken, however, the *WWP1* expression has not been studied. The expression analysis of *WWP1* gene is important since it was reported that altered expression of known responsible gene could lead dystrophic phenotype (Smythe and Rando, 2006).

In this study, we analyzed the mRNA expression of *WWP1* in various skeletal muscles and other tissues of normal and dystrophic chickens by using Northern blotting and reverse transcription (RT)-PCR analysis to know the differences in the general expression pattern between them.

Materials and Methods

Chickens

A two-month-old dystrophic chicken (New Hampshire: NH-413) and an age-matched normal chicken (White Leghorn: WL-F) were used in this study. The New Hampshire (NH-413) strain is a homozygous dystrophic line introduced from University of California, Davis to Japan in 1976 (Kondo *et al.*, 1982). The disease in this strain is transmitted co-dominantly by a single gene, but the phenotype is modified by other background genes (Kikuchi *et al.*, 1981, 1987; Wilson *et al.*, 1979). The White Leghorn (WL-F) strain was established in 1970s, and maintained as closed colony in the Nippon Institute of Biological Science in Yamanashi, Japan. This study was carried out according to the guidelines of Animal Experimentation of Kobe University.

Expression analysis

For Northern blotting, mRNAs were isolated from *M. pectoralis superficialis* (PS), *M. tensor fascia lata* (TFL), *M. biceps femoris* (BF), *M. triceps surae* (TS), *M. peroneus longus* (PL), heart (H), brain (B), liver (L), kidney (K) and whole embryo (E) with PolyATtract mRNA Isolation kit (Promega, Madison, WI, USA). The 2μg of mRNAs, which were measured with NanoDrop ND-1000 spectrophotometer (NanoDrop Technologies, Wilmington, DE, USA), were resolved by 1.2% agarose gel electrophoresis in the presence of formaldehyde and blotted on to Hybond-N+membrane (GE Healthcare Bio-Sciences AB, Uppsala, Sweden). The mRNAs were visualized using digoxigenin (DIG) reagents, and kits for non-radioactive nucleic acid labeling and detection system (Roche Diagnostics, Basel, Switzerland) according to the procedure specified by the manufacturer excepting that the washing was done with 4×SCC 0.1% SDS at room temperature for 10 min, 4×SCC 0.1% SDS at 40℃ for 8 min and then 2×SCC 0.1% SDS at 40℃ for 8 min twice. The DIG-labeled DNA probes were prepared by PCR using DIG-dUTP using pectorals cDNA sample of a WL-F strain female as a template. The primers applied in this procedure were 5′-tccctcataaatgttgaaagcagaca-3′ (WWP1p-F), 5′-gtaataacccaaggtaatatgtaaac-3′ (WWP1 p-R) (NM_001012554), 5′-ccgtgtgccaacccccaatgt ctctg-3′ (GAPDHp-F) and 5′ -cagtttctatcagcctctcccacctc- 3′ (GAPDHp-R) (NM_204305). The PCR was done for 35 cycles at 94℃ for 30 sec, 55℃ for 30 sec, 72℃ for 30 sec (*WWP1*) and for 35 cycles at 94℃ for 30 sec, 63℃ for 30 sec, 72℃ for 30 sec (*GAPDH*) using TaKaRa Ex Taq® Hot Start Version (Takara Bio Inc., Tokyo, Japan). Quantitative analysis was performed with Scion Image (Scion Corporation, Frederick, MD, USA).

In order to analyze mRNA expression of *WWP1* gene in the PS, *M. anterior latissimus dorsi* (ALD) and H, RT-PCR method was applied. The concentration of cDNA derived from these muscles was calculated by NanoDrop ND-1000 (NanoDrop Technologies) and commeasurable cDNAs were used as template. The primers applied were 5′-attaggaagagccactgtagact-3′ (WWP1r-F) and 5′-tctgttgattgaggttctgctgt-3′ (WWP1r-R) (NM_001012554). The PCR was done for 35 and 40 cycles at 94℃ for 30 sec, 56℃ for 30 sec, 72℃ for 30 sec using TaKaRa Ex Taq® Hot Start Version (Takara Bio Inc.).

Histology

The PS, ALD and H were snap-frozen in liquid nitrogen-cooled isopentane and sectioned in a cryostat (Leica Microsystems Japan, Tokyo, Japan). The histopathology was made by hematoxylin-eosin staining (HE) method (Kikuchi *et al.*, 1981).

Results

The mRNA expression of *WWP1* gene was detected by Northern blotting in various muscles and other tissues of normal and muscular dystrophic chickens (Fig. 1). Two bands were detected in all tissues examined, and revealed almost equally expression level in any muscles and tissues observed.

In the PS, BF, TS, PL, B and K, *WWP1* gene was strongly expressed in normal than in dystrophic chickens (Fig. 1). *GAPDH* was used as an internal control of *WWP 1* expression analysis. In TFL, L and E, similar *WWP1* expression level was observed between two phenotypes (Fig. 1).

RT-PCR analysis indicated that *WWP1* gene was expressed in slow tonic ALD, not only in PS and H of both phenotypes (Fig. 2A). Figure 2B shows histopathological changes in PS, ALD and H of normal and dystrophic chickens. The pathological findings in dystrophic PS were characterized by the degenerating fibers with many vacuoles in cytoplasm, the fatty infiltration into connective tissue, and the proliferation of nuclei within muscle fibers with large variation in sizes. However, no such lesions were observed in ALD and H from age-matched dystrophic chickens (Fig. 2B).

Discussion

Northern blotting with *WWP1* specific probe detected two bands in all tissues and muscles examined (Fig. 1). Northern blot analysis of *WWP1* expression in human tissues also exhibited two bands (Mosser *et al.*, 1998), and RT-PCR analysis showed that human *WWP1* gene had at

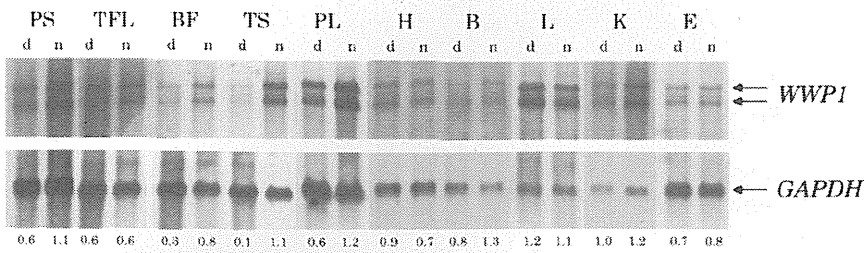

Fig. 1. **Expression of chicken *WWP1* in various tissues.**
A *WWP1* cDNA probe was used to detect *WWP1* mRNA transcripts by Northern blotting using blots containing 2μg of mRNAs from chicken muscles or various other tissues. *M. pectoralis superficialis* (PS), *M. tensor fascia lata* (TFL), *M. biceps femoris* (BF), *M. triceps surae* (TS), *M. peroneus longus* (PL), heart (H), brain (B), liver (L), kidney (K) and embryo (E) were analyzed. A doublet band is detected at variable levels in all tissues. "d" indicates mRNAs from dystrophic chickens. "n" indicates mRNAs from normal chickens. The numbers below the *GAPDH* bands represent the relative ratios of *WWP1/GAPDH*.

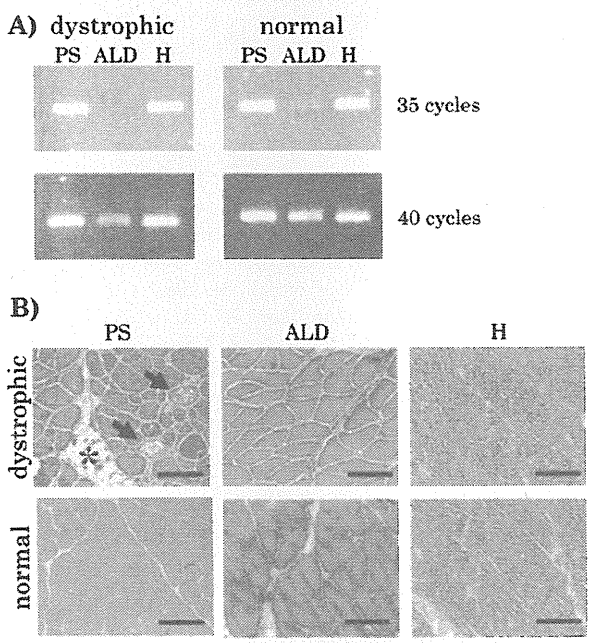

Fig. 2. **RT-PCR detection of *WWP1* gene and histological analysis for three representative muscle types.**
M. pectoralis superficialis (PS), *M. anterior latissimus dorsi* (ALD) and heart (H) expressed *WWP1* less in muscular dystrophic chicken, but only dystrophic PS was severely harmed. A) Expression of *WWP1* in PS, ALD and H was analyzed by RT-PCR method. PCR was performed for 35 or 40 cycles. B) The PS, ALD and H of dystrophic (NH-413) and normal (WL-F) chickens were analyzed with HE staining. Vacuoles (arrows) and fatty infiltration (asterisk) are observed in PS of dystrophic chickens. It is also remarkable that, in dystrophic PS, many muscle fibers have many nuclei in cytoplasm and vary widely in size. These pathological features are not observed in ALD and H of dystrophic chicken. Scale bar=120μm.

least six mRNA isoforms synthesized through the alternative splicing, two of which were strongly expressed and commonly observed in various tissues (Flasza *et al.*, 2002). The mRNA doublet bands of chicken *WWP1* by Northern blot analysis might be equivalent to two bands of human tissues, while a single band was observed by RT-PCR analysis in chicken (Fig. 2A), suggesting that the amplified region does not include alternative spliced site. Flasza *et al.* (2002) also mentioned that the relative ratio of these isoforms from human *WWP1* varied in a tissue-specific manner, but the doublet bands of chicken *WWP1* were expressed almost equally in all tissues examined.

The *WWP1* gene expression in *M. pectoralis superficialis* (PS) of dystrophic chicken was less than that of normal chicken (Fig. 1). The PS of chicken is a fast twitch muscle composed of two types of fast twitch fibers (aW and bW). TFL, BF, TS and PL muscles from wing and leg are mixed muscles co-existing fast twitch (aW and bW) with slow twitch fibers (bR) in a mosaic pattern (Ashmore and Doerr, 1971a), except that the ALD and *M. adductor magnus* are composed of slow tonic fibers (ST) innervated multiply (Ashmore *et al.*, 1978; Kikuchi *et al.*, 1986). In chicken muscular dystrophy, fast twitch fibers are initially and most severely affected, while slow twitch and slow tonic muscles persist relatively harmless throughout the life span (Ashmore and Doerr, 1971b; Barnard *et al.*, 1982). The *WWP1* expression in dystrophic BF, TS and PL showed a similar downward trend as observed in dystrophic PS (Fig. 1). These data indicate that there might not be a causal relationship between the alteration of *WWP1* expression level and the severity of muscular dystrophy, since not only affected muscles but unaffected ones exhibited the same pattern. Moreover, the alteration of *WWP1* expression level was observed in other unaffected tissues, such as B and K, which reinforces our hypothesis that the alteration of *WWP1* expression levels